AD-A049 065 WEIDLINGER ASSOCIATES MENLO PARK CALIF F/G 20/11
EQUIPMENT-STRUCTURE INTERACTION AT HIGH FREQUENCIES.(U)
APR 77 J M KELLY, J L SACKMAN DNA001-76-C-0110
UNCLASSIFIED PR-7702 DNA-4298T NL

1 of 1
ADA049 065

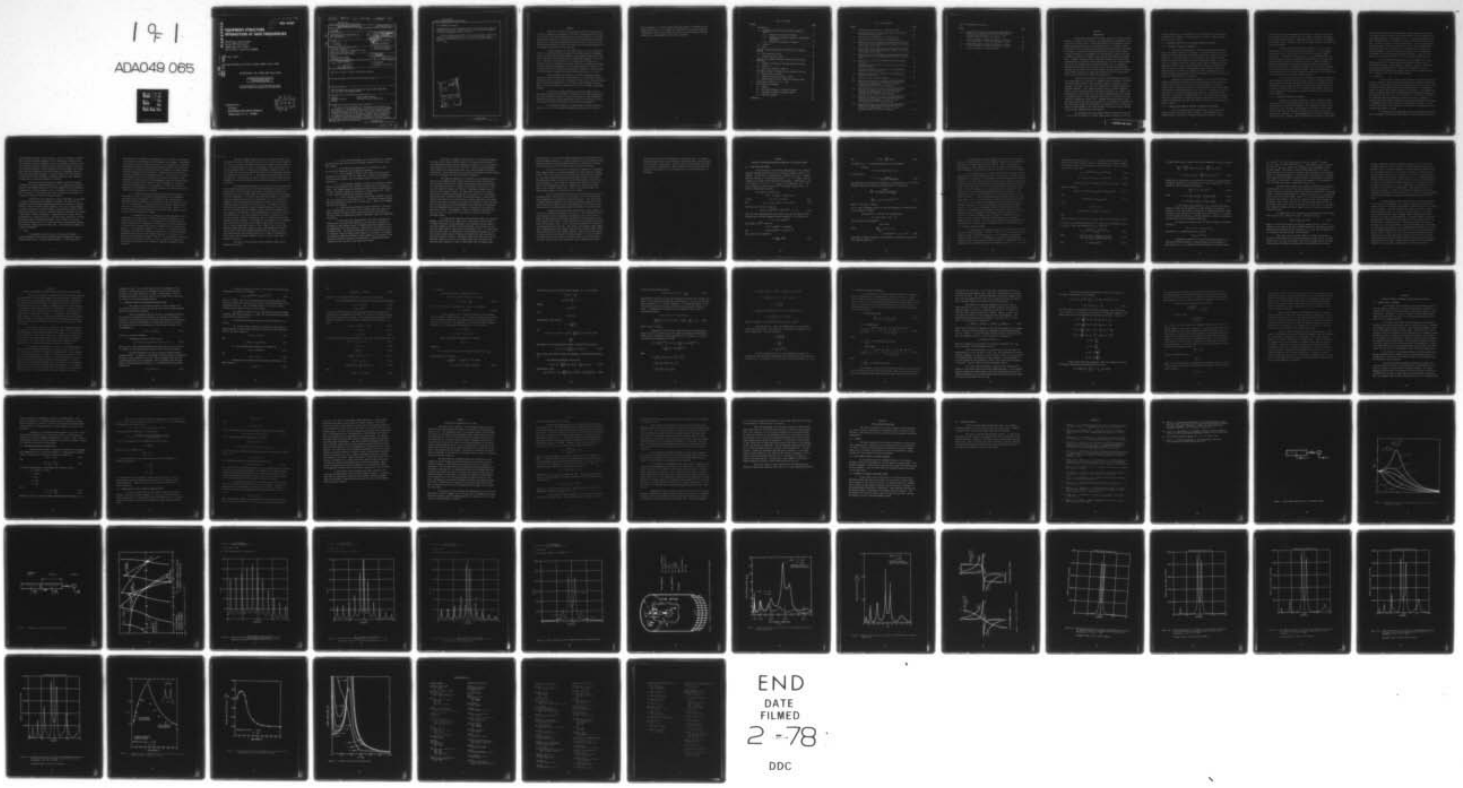

END
DATE FILMED
2-78
DDC

DNA 4298T

EQUIPMENT-STRUCTURE INTERACTION AT HIGH FREQUENCIES

Weidlinger Associates
Suite 245, Building 4
3000 Sand Hill Road
Menlo Park, California 94025

1 April 1977

Topical Report for Period May 1976 — April 1977

CONTRACT No. DNA 001-76-C-0110

THIS WORK SPONSORED BY THE DEFENSE NUCLEAR AGENCY
UNDER RDT&E RMSS CODE B344076462 L19GAXSX33802 H2590D.

Prepared for
Director
DEFENSE NUCLEAR AGENCY
Washington, D. C. 20305

(18) DNA, SBIE (19) 4298T, AD-E300 036

UNCLASSIFIED

SECURITY CLASSIFICATION OF THIS PAGE (When Data Entered)

REPORT DOCUMENTATION PAGE

READ INSTRUCTIONS BEFORE COMPLETING FORM

1. REPORT NUMBER: DNA 4298T
2. GOVT ACCESSION NO.
3. RECIPIENT'S CATALOG NUMBER

4. TITLE (and Subtitle): (6) EQUIPMENT-STRUCTURE INTERACTION AT HIGH FREQUENCIES.

5. TYPE OF REPORT & PERIOD COVERED: (9) Topical Report, May 76—Apr 77,

6. PERFORMING ORG. REPORT NUMBER: (14) PR-7702

7. AUTHOR(s): (10) J. M. Kelly, J. L. Sackman

8. CONTRACT OR GRANT NUMBER(s): (15) DNA 001-76-C-0110

9. PERFORMING ORGANIZATION NAME AND ADDRESS: Weidlinger Associates, Suite 245, Building 4, 3000 Sand Hill Road, Menlo Park, California 94025

10. PROGRAM ELEMENT, PROJECT, TASK AREA & WORK UNIT NUMBERS: Subtask L19GAXSX338-02

11. CONTROLLING OFFICE NAME AND ADDRESS: Director, Defense Nuclear Agency, Washington, D.C. 20305

12. REPORT DATE: (11) 1 April 77

13. NUMBER OF PAGES: 76 (12) 72 p.

14. MONITORING AGENCY NAME & ADDRESS (if different from Controlling Office): (16) L19GAXS, (17) X338

15. SECURITY CLASS (of this report): UNCLASSIFIED

15a. DECLASSIFICATION/DOWNGRADING SCHEDULE

16. DISTRIBUTION STATEMENT (of this Report)

Approved for public release; distribution unlimited.

17. DISTRIBUTION STATEMENT (of the abstract entered in Block 20, if different from Report)

18. SUPPLEMENTARY NOTES

This work sponsored by the Defense Nuclear Agency under RDT&E RMSS Code B344076462 L19GAXSX33802 H2590D.

19. KEY WORDS (Continue on reverse side if necessary and identify by block number)

Dynamics
Equipment Response
Damping
High Frequency Response
Equipment-Structure Interaction

20. ABSTRACT (Continue on reverse side if necessary and identify by block number)

A series of idealized models are considered which incorporate the characteristics of an embedment media, a structure and internal equipment. The equipment has natural frequencies which are high compared with the fundamental frequency of the structure. The purpose of the analysis is to obtain exact solutions to the idealized model. These may eventually be compared with solutions obtained by standard structural dynamics techniques to improve understanding of the degree of refinement needed

DD FORM 1 JAN 73 1473 EDITION OF 1 NOV 65 IS OBSOLETE

UNCLASSIFIED

SECURITY CLASSIFICATION OF THIS PAGE (When Data Entered)

392 150

20. ABSTRACT (Continued)

in modeling and to provide guidance for selecting appropriate numerical integration techniques. Certain results on the vibration of equipment have been obtained which appear to be new.

These techniques are applied to a structure-equipment system using models that are representative of silo-like protective structures. Excitations simulating ground shock, air shock and shaker loading are examined.

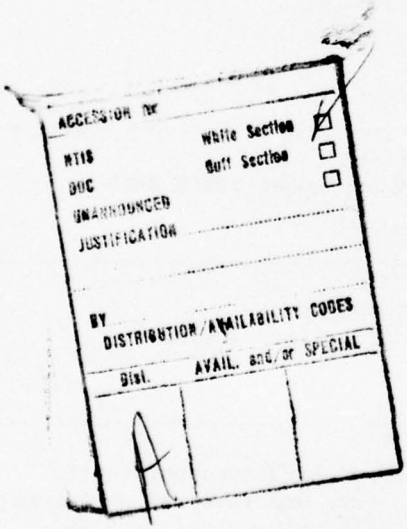

SUMMARY

This report describes certain results obtained in the course of a study of methods for the analysis of the high frequency vibration of structural systems. The main problems which arise are the need for a fine enough spatial discretization to transmit accurately the high frequency vibrations, the need for a suitable time integration algorithm that is accurate for the high frequency range and, finally, the need for an accurate representation of the damping characteristics of the structure.

To gain insight into these problem areas, a series of idealized models are considered which incorporate the characteristics of an embedment media, a structure and internal equipment, the equipment having natural frequencies which are high compared with the fundamental frequency of the structure. The purpose of the analysis is to compare exact solutions to the idealized model with appropriate solutions, which may be obtained by standard structural dynamics techniques to give an understanding of the degree of refinement needed in the modeling and the numerical technique. Certain results on the vibration of equipment have been obtained which appear to be new.

These techniques were applied to a structure-equipment system using more realistic models that are representative of silo-like protective structures and it was shown that essentially the same type of results developed. This shows that the phenomenon is not confined to the elementary idealized model. Excitations simulating ground shock, air shock or shaker loading were examined.

An alternative simple modeling of structural damping is introduced which has much the same degree of simplicity as the usual damping model but leads to improved estimates of structural response at high frequencies. The model is based on the well known Maxwell model of viscoelasticity and in a one degree-of-freedom system requires only one damping parameter.

For sinusoidal loading of a single degree-of-freedom system the response is that of a conventional damping around resonance but differs at

high frequencies. In a multi degree-of-freedom system it is possible to use modal damping factors. It is shown that algorithms for the direct numerical integration of the matrix equations of motion of the multi degree-of-freedom system can be easily adapted to this type of modeling.

TABLE OF CONTENTS

LIST OF ILLUSTRATIONS

LIST OF ILLUSTRATIONS (Continued)

SECTION 1

INTRODUCTION

Conventional methods for the dynamic analysis of large structural systems are designed to be accurate in the computation of the response of the system for the lowest modes. In most applications, as for example in earthquake engineering design, only the low-mode response is of interest and in these cases the use of implicit unconditionally stable integration algorithms is preferred. In addition to being unconditionally stable, when low-mode accuracy is needed it is advantageous for an algorithm to possess some form of numerical dissipation to damp-out any spurious participation from higher modes. Commonly used algorithms in structural dynamics which possess these characteristics are Houbolt's method (Reference 1), Wilson's θ method (Reference 2) and the Newmark family of methods (Reference 3). In earthquake engineering these methods are justified on the basis that the higher-mode response does not affect the structural design. Another reason for suppressing the higher frequencies is that size limitation forces a discretization which does not reproduce the higher modes accurately.

There are many situations in which the high frequency response of a structure might be of interest, for example it may be necessary to estimate the accelerations induced in non-structural elements in buildings, such as equipment or ordinance and it may also be necessary to design mountings for sensitive equipment. Most computer programs used by structural designers utilize a fairly crude modeling of the system considering, for example, only three degrees of freedom per story and modeling damping using either viscous or hysteretic models. These techniques are accurate in a typical structural frame up to frequencies around 10 Hz. Equipment design and design of non-structural elements may require techniques which are accurate to around 200 Hz. The conventional model will thus operate as an analytical filter and prevent energy at high frequencies from being included in the motion of the relevant non-structural components during the analysis.

The research work in this Report describes results which are important in the development of suitable computational techniques to allow the

accurate computation at a reasonable cost of the response of non-structural components and equipment in structures subject to dynamic loading produced by ground and air shock.

1.1. BACKGROUND--DIFFICULTIES WITH CURRENT METHODS OF ANALYSIS

1.1.1. PROBLEMS OF MESH SIZE UNIFORMITY

The finite element method is the most popular technique now in use for the dynamic analysis of structures. In conjunction with large computers the method offers great flexibility and accuracy. However, if three-dimensional structural behavior is to be included, an analysis using this method will require much computer time and considerable expense. To reduce the cost of computer time, many current programs employ assumptions of floor diaphragm rigidity and also neglect inertia at column-floor intersections which, with the use of static condensation, greatly reduce the number of dynamic degrees of freedom to be considered. These assumptions are very useful in reducing the computer time of the analysis but then also reduce the frequency transmissibility of the model.

Modeling the high frequency response of a structure using finite element methods requires elements to be small and leads to large numbers of elements and equations of motion and to related problems of storage and computer time. Experience in the use of codes designed to solve wave propagation problems has shown (References 4 and 5) that it is essential to select a mesh which is as spatially homogeneous as possible to avoid spurious back reflections from regions of changing mesh size. This means that refining the mesh in the neighborhood of points of interest becomes impractical for high frequency problems and that some other method of reducing the storage requirements is needed.

1.1.2. PROBLEMS WITH NUMERICAL DAMPING IN INTEGRATION ALGORITHMS

In most structural dynamics applications, the use of implicit unconditionally stable algorithms is favored. Such algorithms are the Newmark family of operators, the Houbolt method and the Wilson θ method.

These algorithms all provide numerical dissipation to damp out any previous participation of higher mode response. The amount of numerical dissipation is controlled by the time step. Reducing the time step reduces the damping in each mode. Thus, to ensure accuracy in the higher modes, a very small time step may be needed.

In the Wilson θ method, the only parameter, θ, must be taken greater than 1.37 to maintain unconditional stability. It is recommended (Reference 2) that θ be taken to be 1.4 for which the method is highly dissipative. To integrate a mode accurately, it is recommended that 100 steps be used per period. This would seem to indicate that extremely small time steps would be needed for high modal accuracy. Houbolt's method is generally considered to be even more dissipative than the Wilson method and the Newmark family is considered (Reference 6) to be even more dissipative than both the Wilson and Houbolt methods. Thus, the Wilson method is considered by many to be the best available unconditionally stable algorithm, but is clearly unsuited for high frequency analysis.

The small time step and fine discretization needed for high frequency analysis by implicit analysis brings a number of attendant problems. These are mainly concerned with the matrix inversions associated with time integration schemes, which will lead to extremely large generalized stiffness matrices and may make the use of current implicit methods impractical. It also suggests the possible use of explicit methods which do not involve matrix inversions.

1.1.3. PROBLEMS WITH MODELING OF DAMPING

Damping of structural vibrations is almost invariably treated according to the viscous damping model in which viscous resisting forces (proportional to velocity) are assumed to act alongside the elastic restoring forces of the structure. One advantage of this model is great mathematical simplicity; the equations of motion are very easy to set up and, under certain conditions, to solve provided that the matrix of damping coefficients is known. However, these coefficients are not directly measurable;

they can only be inferred from measurements of modal damping ratios (since it is these ratios that determine the amplification factor at resonance, the logarithmic decrement of free vibrations, etc.). Experiments generally show that the damping ratio in a homogeneous structure varies little from mode to mode. On the other hand, the viscous damping model, with the damping coefficients regarded as material properties of the structural elements (much as the elastic properties), predicts that the damping ratio increases with natural frequency. Thus, the high frequency modes tend to be damped out (independently of the aforementioned numerical damping). Therefore, this model is not particularly suited to the study of high frequency motion.

A mode-independent damping ratio may be assumed in the viscous damping model only if the mode-superposition method is used and this is practicable only with a limited number of degrees of freedom. Other models of structural damping include the "hysteretic" (Reference 7) and the Rosenblueth-Herrera (Reference 8) models, both nonlinear, and hence difficult to apply to multi degree-of-freedom systems.

1.2. OBJECTIVE

In this section certain results obtained in preliminary investigations of methods for the high frequency vibrations of structural systems are described. To gain insight into the problems which arise in this area a series of idealized models which incorporate the characteristics of an embedment medium, a structure and internal equipment was considered. The equipment has natural frequencies which are high compared with the fundamental frequency of the structure. The objective of this analysis is to compare exact solutions to the idealized model with appropriate solutions which may be obtained by standard structural dynamics techniques to give an understanding of the degree of refinement needed in the modeling and the numerical technique. In the course of this study, certain results on the vibration of equipment have been obtained which appear to be new.

The combined structure-equipment systems considered here are such that the equipment is relatively light and has a natural frequency much above

the fundamental frequency of the structure. This is in contrast to earlier work of Geers and DeRuntz (Reference 9), for example, who consider structural systems, typical of submarines, where the equipment is massive, may in fact be heavier than the structure, and has a natural frequency lower than the structural frequency. Three systems have been considered, two of which while idealized incorporate the characteristics of an embedment medium, a structure, and attached equipment. The third model is more representative of silo-like structures involving an embedded cylindrical shell capped by a circular plate to which the equipment is attached.

Results presented here appear to suggest conclusions somewhat different from previous investigations such as, for example, Scavuzzo (Reference 10) and Newmark (Reference 11) who have suggested that the problem of equipment with a natural frequency close to a frequency of the structure is not a serious one. The present results indicate that such a situation, referred to as "tuning," may in fact be quite serious.

A deficiency of the analysis for these three models is the neglect of material damping (radiation damping is included). One objective is to incorporate into the analysis damping models which are realistic at high frequencies. Many of the difficulties attendant on the use of viscous damping in structural analysis of impact problems or high frequency analysis can be alleviated by the use of general viscoelastic models to represent the response of the system. However, the degree of complication which results could be considerable for a large system, and it would be almost impractical to obtain the necessary data to define the response. What is needed is some model which has the simplicity of the viscous model which can be generally defined by specifying a damping factor for each mode. In this Report one example of a model is described.

1.3. SCOPE

To accomplish these objectives, the interaction between a structure-foundation system and an attached item of equipment has been considered through the use of simple idealized models. In the first model a

semi-infinite rod represents the foundation or soil, a finite rod represents the structure and a spring-mass system represents the equipment. The purpose of the analysis, given in detail in Section 2 is to determine the acceleration amplification factor of the mass representing the equipment when the system is subject to an enforced oscillatory input of frequency ω at large distances from the foundation-structure interface. The amplification factor at any frequency ω depends on the following parameters: γ--the ratio of the mass of the equipment to that of the structure, ω_o--the natural frequency of the equipment on a fixed support, ω^*--the fundamental frequency of the structure on a fixed foundation and a parameter R which determines the reflection-transmission characteristics of the interface. A value of R less than 1 means that an unloading wave is reflected back into the medium, greater than 1 means that a loading wave is reflected.

To estimate its value an unbraced frame building located on a soil medium in which a horizontally polarized shear wave is propagating vertically has been considered. As an example of such a building, the building discussed in Reference 12 on an alluvial soil was used and a value of R = 0.1 was obtained. An unbraced frame is a relatively flexible structure, for a stiffer building the value of R would increase. When R = 1, a wave is transmitted without change into the structure, the structure acting in effect as an extension of the medium.

The amplitude factor as a function of forcing frequency ω for a system with R = 0.1 was found to have the following characteristics. For small values of the mass ratio, γ, the resonances of the system below the natural frequency of the equipment are shifted below the natural frequencies of the structure alone and those above are shifted above the structure frequencies. If the equipment frequency is not close to a structure frequency, an additional resonance is interpolated between those structural frequencies immediately above and below the equipment frequency. The results for an untuned system are shown in Figures 5a and 5b. In these figures the amplification factor is shown for a case where R = 0.1 and the natural frequency of the equipment lies between 4 and 5 times the fundamental frequency of the structure.

When the equipment resonance falls on a structure resonance (i.e., the system is tuned), a double peak occurs with the two maxima close together. It is easy to show that the distance between the two peaks is proportional to $\sqrt{\gamma}$. An interesting point is that if the equipment is not tuned to the structure the dominant peak is virtually at the equipment resonance; however, if it is tuned, the value of the amplification factor at the equipment frequency is reduced and is proportional to γ. The peaks on either side, however, are now important. These results are shown in Figure 6a and also Figure 6b as an expanded curve near the equipment resonance when the equipment mass ratio is very small.

This double peak corresponds to the occurrence of two simple poles of the system transfer function in the transform domain being very close together and, in the case of very light mass, to essentially a double pole. The implications of this double peak on the transient response of the system could be considerable. It is easy to show that the presence of a double pole leads to transient build-up which is proportional to t^2 in a condition of resonance. The tuned situation thus appears to be more critical even than normal resonance, in contrast to earlier results. For example, Scavuzzo (Reference 10) using somewhat similar modeling involving an infinite bar to which a cantilevered mass was attached, found by numerical techniques that the response at the frequency of the vibrating mass is less when the mass is tuned than when it is not and concluded that tuning is, therefore, not a critical situation. Herein the identical result is obtained but the interpretation is quite different. The response at the frequency of the equipment when the system is not tuned is very large and when tuned, is much less. This is clearly indicated in Figures 5 and 6. However, the fact is that a numerical method might well overlook the very large amplification factors on each side of the tuned equipment frequency when the system is tuned. These twin peaks may lead to amplification over a range of frequencies on either side of the equipment frequency, thus presenting a large target to resonant conditions.

The results of this analysis on the elementary models may be summarized as follows:

a. In the structure-equipment case, the frequencies of the system are shifted such that those below the equipment frequency are lower, those above higher.

b. As the mass ratio becomes small, the frequencies tend to the structural frequencies and the equipment frequency.

c. If the equipment frequency is not tuned to the structural frequencies, the response curve for light mass is roughly the superposition of the structural response and the equipment response curves with little interaction.

d. If the equipment frequency is tuned to a structural frequency, there are two frequencies close together on either side of the tuning frequency. The response magnitude intermediate between these is proportional to $1/\gamma$ while the spread between the frequencies is proportional to $\sqrt{\gamma}$. There is thus a spread of high amplification over that band.

e. In the transient problem the double peak resonance is equivalent to a multiple pole in the limit as $\gamma \to 0$. The resonant response around the tuning frequency will grow like t^2 rather than t. Thus, in the undamped case this will dominate.

f. Since the spread between the peak frequencies in the tuned case is proportional to the square root of the mass ratio, the effect is a band of resonant frequencies which vanishes slowly with decreasing mass ratio and, thus, for light masses offers a substantial target for sympathetic oscillation.

A third model more representative of silo-like structures was analyzed and it was found that essentially the same type of response is developed in more realistic models of equipment-structure systems and that the phenomenon of the double peak in a tuned system is not confined to the elementary model. The structure considered here is illustrated in Figure 7. It comprises a long cylindrical shell topped by a flat plate. To maintain the analytical simplicity afforded by axial symmetry in the response of the plate and cylinder the equipment is idealized as a spring-supported mass connected to the structure at the center of the plate.

The system is assumed to be excited by: (a) sinusoidal displacement input at the base of the shell which is far removed from the plate; or (b) sinusoidally varying pressure loading on the plate; or (c) an oscillatory point load applied to the center of the plate. These excitations maintain axial symmetry and simulate ground shock, air shock and shaker excitations, respectively. Other cases which do not possess axial symmetry could be treated but with a substantial increase in analytical complexity.

The algebraic complexity of the analysis is considerably greater than for the elementary models studied in the earlier report and the fact that the plate is governed by a fourth order equation while the bar equation is second order gives rise to a number of differences in the results. However, the essential features are the same. The double resonance occurs as before when the system is tuned. The double peak resonance is as before dominant in the amplification diagram and it is found that as the equipment mass becomes small the spread between the peaks decreases at a rate proportional to the square root of the mass ratio. Results derived for the spread between the peaks as a function of the structure frequency to which the equipment is tuned indicate that the phenomenon is more important at frequencies above the fundamental and the effect appears to decrease at very high frequencies of tuning. The phenomenon is thus an intermediate frequency one in this case, but it is clear that it may arise in a variety of structure-equipment systems.

To accomplish the objective of incorporating simple, but realistic damping, a model based on the simple linear viscoelastic material known as the Maxwell material has been developed. The conventional viscous model of structural damping is analogous to the Kelvin model of viscoelasticity and the other simple model is that denoted as the Maxwell model. It is well known that the Kelvin model is inadequate for wave propagation problems since the model cannot transmit waves; it implies an infinite wave speed and leads to parabolic equations of motion. The Maxwell model on the other hand leads to hyperbolic equations of motion and transmits waves with the elastic wave speed and some attenuation. Thus, it seems likely that the Maxwell model

when converted to the structural problem might be useful for impact problems and high frequency analysis. It should be noted that the same number of parameters are needed to define the Maxwell model as are needed for the Kelvin model and that the use of modal damping factors would also suffice.

The most effective way to illustrate the behavior of the damping model suggested here is to study the response of a single degree-of-freedom system. This is done in detail in Section 4 where the steady state response of a one degree-of-freedom system under sinusoidal loading is determined. The steady state dynamic load factor, that is displacement per unit load, is shown in Figure 14. In the region of resonance the response is similar to that for Kelvin damping but near zero frequency the result grows without bound as the frequency tends to zero. This is to be expected since the Maxwell model behaves as a fluid under static loading.

For a multi degree-of-freedom system, the equations of motion for the Maxwell model can be put into the same form as those for conventional viscous damping with a modified forcing function vector. This implies that a computer program designed for the conventional dynamic analysis of structural systems can be employed with slight modification for the same type of problem but with the damping represented by the Maxwell viscoelastic model.

A significant difference that exists between the two models is in the initial conditions which need to be specified. The conventional viscous model requires that the displacement and velocity at the initial time be known and these quantities completely determine the initial internal forces. With a Maxwell model, however, these quantities do not determine the initial value of the internal force. In fact, this must be specified in addition to the displacement and the velocity. This aspect of the Maxwell model suggests that it might indeed be more suitable than the Kelvin model for impact problems and similarly for high frequency analysis. While a structural system at rest acquires an initial velocity following an impact, it is not reasonable to assume that this also results in non-zero values for resisting forces. The use of a Kelvin model does incorporate such an assumption and leads to

high accelerations and low displacements in the higher modes. In contrast, the Maxwell model results in more flexible response and gives lower accelerations and higher displacements. With mass proportional damping, modal damping is inversely proportional to modal frequency and both models give essentially the same answers for the low damping ratios resulting from such an assumption.

SECTION 2

ANALYSIS OF EQUIPMENT-STRUCTURE INTERACTION IN IDEALIZED SYSTEMS

2.1. FIRST ANALYTICAL MODEL

As an approach to a qualitative understanding of the problem of equipment response to ground shock, the following elementary model is considered. The structure is represented by a uniform rod of area a, Young's modulus E, density ρ of semi-infinite extent $-\infty < x < 0$ to which a mass m is attached by a spring k which represents the equipment. Displacement of the rod is given by u (x, t), $-\infty < x < 0$, and of the equipment by w (t). The rod is subject to a forced motion $u_o e^{i\omega t}$ at distances remote from x = 0. Figure 1 illustrates the system.

The equations of motion are

$$m\ddot{w} = -F \quad \text{where } F = k(w-u(o,t)),$$

so that

$$m\ddot{w} + k\,w = k\,u(o,t), \tag{2-1}$$

and

$$\rho\, u_{,tt} = E\, u_{,xx} \quad \text{with } F = E\, a\, u_{,x}(o,t). \tag{2-2}$$

The solution in the rod is given by

$$u(x,t) = Ae^{i\omega(t+x/c)} + Be^{i\omega(t-x/c)};\ c^2 = E/\rho \tag{2-3}$$

the first term representing the ground shock input and the second the back reflected wave from the equipment structure interface. It follows that

$$F = E\, a\, i\omega/c\ (A-B)e^{i\omega t}$$

and taking $w = We^{i\omega t}$ results in

$$(-m\omega^2 + k)We^{i\omega t} = k\ (A+B)e^{i\omega t}$$

and

$$E\, a\, i\omega/c(A-B)e^{i\omega t} = k\ \{A+B-W\}\ e^{i\omega t}$$

Thus, there are two equations

$$W = \frac{k}{k-m\omega^2}\ (A+B) \tag{2-4}$$

and

$$W = A+B - \frac{iEa\omega}{kc}(A-B) \tag{2-5}$$

relating W, A, B. A is assumed known and W to be determined.

Defining

$$D = 1/(1-\omega^2/\omega_o^2) \text{ with } \omega_o^2 = k/m$$

it follows that

$$W = -2i \frac{Ea\omega/kc}{(1-1/D) - i\, Ea\omega/kcD} A \tag{2-6}$$

The comparison of the maximum acceleration of the equipment, i.e, ω^2 W to the maximum acceleration induced by the ground shock ω^2 A is given by

$$\left|\frac{W}{A}\right| = \frac{2\alpha\omega/\omega_o}{\{(1-1/D)^2 + \alpha^2\, \omega^2/\omega_o^2 D\}^{1/2}}$$

or

$$\left|\frac{W}{A}\right| = 2\,\alpha\,\{\Omega^2 + \alpha^2(1-\Omega^2)^2\}^{-1/2} \tag{2-7}$$

where $\Omega = \omega/\omega_o$ and $\alpha = \rho ac/m\omega_o$.

(α is a sort of impedance ratio, or could be interpreted as a mass ratio if c/ω_o is taken as a length.

The function $\Omega^2 + \alpha^2(1-\Omega^2)^2$ has a minimum where

$$\Omega^2 = (2\alpha^2-1)/2\alpha^2 \quad \text{if } \alpha^2 > 1/2$$

and the value of this minimum is

$$(4\alpha^2-1)/4\alpha^2$$

Thus,

$$\left|\frac{W}{A}\right|_{max} = 2, \ \alpha^2 < 1/2$$

$$= 4\alpha^2/(4\alpha^2-1)^{1/2} \quad \text{if } \alpha^2 > 1/2 \tag{2-8}$$

This result is shown in Figure 2 in which $|W/A|$ is plotted as a function of Ω for various values of α.

The conclusion is that the amplification factor has its maximum value at a frequency shifted below the equipment frequency and that amplification tends to a maximum value of 2α for large α. Large α corresponds to light equipment; thus, amplification can be very large for light equipment. The disadvantages of this model are that the structure is not clearly defined.

It is interesting to note that this result has an analogy with the single degree-of-freedom damped oscillator. The mass ratio α in this analysis corresponds to $1/(2\xi)$ where ξ is the fraction of critical damping in the damped oscillator. The amplification factors in the two cases differ by a factor of 2, which arises in the present case due to the doubling (caused by wave reflections) at the right end of the bar of the motion imposed at the left end of the bar. Critical damping, $\xi = 1$, corresponds here to a mass ratio $\alpha = 1/2$, at which value the free vibration response becomes non-oscillatory. The amplification factor at any frequency ratio Ω is less than that at zero frequency for values $\alpha < 1/\sqrt{2}$ even though the free vibration response is oscillatory when $\alpha > 1/2$. It is also useful to note that the amplification factor at $\Omega = 1$, i.e., at resonance of the undamped system, is less than the zero frequency value when $\alpha < 1$, which corresponds in the analogy to a damping ratio of $\xi = 1/2$. Thus, in resonance testing of buried structures where interest is concentrated on the frequency ratio near the resonance of the unburied structure, the resonance of the buried structure would appear to vanish for an effective damping ratio of around 1/2, equivalent to a mass ratio of around 1.0, even though this buried system has an oscillatory response in free vibration. This may be an explanation for the unanticipated disappearance of resonance peaks in resonance testing of buried structures.

2.2. ADVANCED ANALYTICAL MODEL

A disadvantage of the previous model is that the mass of the structure is not easily specified. In order to obtain a definite structure mass, a model in which a semi-infinite rod, $-\infty < x < 0$, represents the embedment medium, a finite rod $0 < x < \ell$ represents the structure and a spring mass system represents the equipment as shown in Figure 3 is considered. The displacement of the semi-infinite rod will be denoted by $u_1(x,t)$, $-\infty < x < 0$, that

of the finite rod by $u_2(x,t)$, $0 < x < \ell$. As before the displacement of the mass will be denoted by $w(x,t)$, and it is assumed that the system is subject to an enforced input at large distances from the interface. Thus, the solution involves three parts:

$$u_1 = A_1 e^{i\omega(t-x/c_1)} + B_1 e^{i\omega(t+x/c_1)} \tag{2-9}$$

$$u_2 = (A_2 \sin \omega x/c_2 + B_2 \cos \omega x/c_2) e^{i\omega t} \tag{2-10}$$

$$m \ddot{w} + k w = k u_2(\ell,t), \text{ where } c_1^2 = E_1/\rho_1,\ c_2^2 = E_2/\rho_2 \tag{2-11}$$

with the conditions

$$u_1(0,t) = u_2(0,t);\ E_1 a_1 u_{1,x}(0,t) = E_2 a_2 u_{2,x}(0,t) \tag{2-12}$$

and

$$k\,(w-u_2(\ell,t)) = E_2 a_2 u_{2,x}(\ell,t) \tag{2-13}$$

Thus,

$$A_1 + B_1 = B_2$$

$$E_1 a_1(-i\omega/c_1 A_1 + i\omega/c_1 B_1) = E_2 a_2 \omega/c_2 A_2$$

and

$$kW-k\,(A_2 \sin \omega\ell/c_2 + B_2 \cos \omega\ell/c_2) = E_2 a_2\{\omega/c_2 A_2 \cos \omega\ell/c_2 - \omega/c_2 B_2 \sin \omega\ell/c_2\}$$

As before, A_1 is assumed specified and W is solved for by elimination of B_1, A_2, and B_2. After much manipulation, it is found that:

$$W = 2D \frac{\sin \omega\ell/c_2 + \Gamma \cos \omega\ell/c_2}{\Gamma + iR} A_1 \tag{2-14}$$

where

$$\Gamma = \frac{(D-1) \sin \omega\ell/c_2 - E_2 a_2 \omega/kc_2 \cos \omega\ell/c_2}{(1-D) \cos \omega\ell/c_2 - E_2 a_2 \omega/kc_2 \sin \omega\ell/c_2} \tag{2-15}$$

and

$$R = E_2 a_2 c_1 / E_1 a_1 c_2. \tag{2-16}$$

The amplification factor, namely, the absolute magnitude of W/A_1, is given by

$$\left|\frac{W}{A_1}\right| = 2\,\frac{E_2 a_2 \omega}{k c_2}\,\{((D-1)\,\sin\,\omega\ell/c_2 - \frac{E_2 a_2 \omega}{k c_2}\,\cos\,\omega\ell/c_2)^2$$

$$+ R^2\,((1-D)\,\cos\,\omega\ell/c_2 - \frac{E_2 a_2 \omega}{k c_2}\,\sin\,\omega\ell/c_2)^2\}^{-1/2} \qquad (2\text{-}17)$$

Noting that the total mass of the structure M is given by $\rho_2 \alpha_2 \ell$ and that the fundamental frequency of the structure ω^* is $\pi c_2/2\ell$ a mass ratio $\gamma = m/M$ is introduced finally yielding the expression

$$\left|\frac{W}{A_1}\right| = 2\,\{P^2 + R^2\,Q^2\}^{-1/2} \qquad (2\text{-}18)$$

where

$$P = (1-\omega^2/\omega_o^2)\,\cos\,\frac{\pi}{2}\,\frac{\omega}{\omega^*} - \gamma\,\frac{\pi}{2}\,\frac{\omega}{\omega^*}\,\sin\,\frac{\pi}{2}\,\frac{\omega}{\omega^*} \qquad (2\text{-}19)$$

$$Q = (1-\omega^2/\omega_o^2)\,\sin\,\frac{\pi}{2}\,\frac{\omega}{\omega^*} + \gamma\,\frac{\pi}{2}\,\frac{\omega}{\omega^*}\,\cos\,\frac{\pi}{2}\,\frac{\omega}{\omega^*} \qquad (2\text{-}20)$$

In this equation the parameters γ, ω_o, ω^* can be easily given numerical values, but the parameter R is more difficult to determine. To estimate its value the example is considered of a shear building with column stiffness k, story masses m, story height h and story module b x d, located on a soil medium with density ρ_s and shear modulus G_s in which a horizontally polarized shear wave is propagating vertically.

The equation of motion for the i^{th} mass of a module of the shear building is

$$m\,\ddot{u}_i = -\,2k\,u_i + k\,u_{i+1} + k\,u_{i-1}$$

which leads to a continuum equation of the form

$$m\,u_{,tt} = k\,h^2\,u_{,xx}$$

Dividing both sides by b d h gives an equivalent density ρ_b = m/bdh and equivalent modulus E_b = 2kh/bd and thus in the parameter R = $E_2 a_2 c_1/E_1 a_1 c_2$, E_1, c_1 is replaced by the shear modulus G_s and shear speed

$c_s = (G_s/\rho_s)^{1/2}$ of the soil and E_2, c_2 by E_b and $c_b = (E_b/\rho_b)^{1/2}$ and take $a_1 = a_2$. Thus, $R = kh/bd\ (m/kh^2)^{1/2}/G_s c_s$. An alternative form is to write R in the form $\rho_b c_b/\rho_s c_s$, and utilize information on the fundamental period of the structure. For example, a shear building (Reference 12) of total height 230 feet has a period of 2.2 seconds. The wave speed is thus 400 feet/second. The equivalent density of this building is estimated to be 50 pounds/feet^3 based on a story weight of 250,000 pounds, a story height of 12 feet and a 20 feet by 20 feet module. Considering a soil density of 100 pounds/feet^3 and a soil shear wave speed of 2,000 feet/second, R = 0.1.

The number R determines the reflection transmission characteristics of the interface. A value of R less than 1 means that an unloading wave is reflected back into the medium, greater than 1 means a loading wave is reflected. A shear or unbraced frame building is a flexible structure; for a stiffer building the value of R would increase. When R = 1, a wave is transmitted without change into the structure, the structure acting in effect as an extension of the medium. Thus, in the case of R = 1, the result should reduce to that of the earlier model, and it is easy to see that it, in fact, does. It is, therefore, useful to consider the case of small R since for R near 1 the previous results will hold.

For small values of R the peaks of the amplification function $|W/A_1|$ will be close to the zeroes of the term P. These are given by

$$\frac{\pi}{2}\frac{\omega}{\omega^*} \tan \frac{\pi}{2}\frac{\omega}{\omega^*} = \frac{1}{\gamma}\,(1-\Omega^2) \qquad (2\text{-}21)$$

When m = 0, the zeroes are those of $\cos \frac{\pi}{2}\frac{\omega}{\omega^*}$, namely $(2n-1)/2\ \pi$, which correspond to a bar fixed at one end and free at the other. The zeroes for finite values of m are shifted lower for those below $\omega = \omega_o$ (the natural frequency of the equipment) and shifted higher for those above.

When x tan x and $1/\gamma\ (1-\beta^2 x^2)$ where $\beta = 2\omega^*/\pi\omega_o$ are plotted it is seen that the zeroes of P are the intersections of these curves. For small values of m, it is clear from Figure 4 that for the untuned case of the three zeroes nearest the equipment resonance one is slightly below the structure

resonance immediately below the equipment resonance, one is close to the equipment resonance and one is slightly above the structure resonance immediately above the equipment resonance. When the equipment resonance falls on a structure resonance (i.e., the system is tuned), a double root occurs with two intersections very close together. It is easy to show that the distance between the two roots is proportional to $\sqrt{\gamma}$. An interesting point is that if the equipment is not tuned to the structure the dominant peak is virtually at the equipment resonance; however, if it is tuned, the value of the amplification factor at $\omega = \omega_o$ is reduced and is proportional to $1/\gamma$. The peaks on either side are now important. These results are shown in Figures 5, 6a and 6b. In Figure 5 the result is shown when the system is not tuned and in Figure 6a the result when it is. Figure 6b shows an expanded curve near the equipment resonance when the equipment mass ratio is very small.

The implications of this double root on the transient response of the system are considerable. It is easy to show that the presence of a double root leads to transient buildup which is proportional to t^2 in a condition of resonance. The tuned situation thus appears to be more critical even than normal resonance in contrast to earlier results. For example, Scavuzzo (Reference 10), using a somewhat similar modeling involving an infinite bar to which a cantilevered mass is attached, found by a numerical technique that the response at the frequency of the vibrating mass is less when the mass is tuned than when it is not and concluded that tuning is, therefore, not a critical situation. The result obtained here is the same; the response at the frequency of the equipment when the system is not tuned is very large and when tuned is much less. This is clearly indicated in Figures 5 and 6. However, the fact is that a numerical method might well overlook the very large amplification factors on each side of the tuned equipment frequency when the system is tuned. These twin peaks may lead to amplification over a range of frequencies on either side of the equipment frequency, thus presenting a larger target to resonant conditions.

SECTION 3

ANALYSIS OF EQUIPMENT-STRUCTURE INTERACTION IN SILO-LIKE STRUCTURES

This section describes the application of the techniques developed in the previous section on high frequency structure-equipment interaction to the vibration of an equipment-structure system which is more representative of silo-like protective structures. The purpose of this is to show that essentially the same type of response is developed in more realistic models of equipment-structure systems and that the phenomenon of the double peak in a tuned system is not confined to the elementary model. The structure considered here is illustrated in Figure 7. It comprises a long cylindrical shell topped by a flat plate. To maintain the analytical simplicity afforded by axial symmetry in the response of the plate and cylinder the equipment is taken to be a spring supported mass connected to the structure at the center of the plate.

The system is taken to be excited by: (a) sinusoidal displacement input at the base of the shell which is far removed from the plate; or (b) sinusoidally varying pressure loading on the plate; or (c) an oscillatory point load applied to the center of the plate. These excitations maintain axial symmetry and simulate ground shock, air shock and shaker excitations, respectively. Other cases which do not possess axial symmetry could be treated, but with a substantial increase in analytical complexity.

The algebraic complexity of the analysis is considerably greater than for the elementary models studied in the earlier report and the fact that the plate is governed by a fourth order equation while the bar equation is second order gives rise to a number of differences in the results. However, the essential features are the same. The double resonance occurs as before when the system is tuned. The double peak resonance is as before dominant in the amplification diagram and it is found that as the equipment mass becomes small the spread between the peaks decreases at a rate proportional to the square root of the mass ratio. Results have also been derived between the peaks as a function of the structure frequency to which the

equipment is tuned. These results indicate that the phenomenon is more important at frequencies above the fundamental and the effect appears to decrease at very high frequencies of tuning. The phenomenon is thus an intermediate frequency one in this case, but it is clear that it may arise in a variety of structure-equipment systems.

3.1. GOVERNING EQUATIONS OF EQUIPMENT-STRUCTURE SYSTEM

The system to be considered consists of three elements, the semi-infinite cylindrical shell, the circular plate and the spring supported mass which simulates the equipment.

The plate equations used here are those of elementary Kirchhoff plate theory; all quantities are assumed to be functions of the radius r and time t. The surface tractions on the plate are positive in the direction of positive transverse displacements w of the middle surface of the plate. The transverse shear force is denoted by Q_r and is given in terms of the displacements by

$$Q_r = - D_p (\nabla^2 w)_{,r} \tag{3-1}$$

where D_p is the plate stiffness.

The equation of motion for the plate is

$$D_p \nabla^4 w (r,t) + \mu_p \ddot{w} (r,t) = p (r,t), \quad r > 0 \tag{3-2}$$

where p (r,t) is the externally applied distributed load on the plate which is intended to approximate airblast effects on the surface of the plate.

The shell equations to be used are based on axially symmetric membrane behavior. In addition, the influence of lateral inertia is neglected. The shell is also considered to be very rigid in bending so that only its longitudinal behavior is of consequence. This also implies that the plate edge is constrained against rotation, i.e., one appropriate plate boundary condition is

$$w_{,r} (a,t) = 0. \tag{3-3}$$

In order to simulate the effect of ground shock the longitudinal displacement of the shell is given by

$$u_s = A_s e^{i\omega(t+x/c_s)} + B_s e^{i\omega(t-x/c_s)} \tag{3-4}$$

where $c_s = \sqrt{E_s/\rho_s}$. The first term represents the prescribed ground shock input at the shell base and the second the back reflected disturbance at the plate-shell interface. When the problem relates to air shock or shaker excitation on the plate the first term is omitted.

The equipment is taken to be a single degree-of-freedom undamped oscillator with natural frequency $\omega_o = \sqrt{k/m}$. The force between the equipment and the plate is denoted by f(t).

The interaction equations between the various elements are as follows:

(a) The shell-plate interaction is governed by continuity of displacement and a balance between the plate edge shear and the longitudinal force in the shell, leading to

$$w\ (a,t) = u_s\ (0,t) \tag{3-5}$$

and

$$Q_r\ (a,t) = E_s\ u_s'\ (0,t)\ t_s \tag{3-6}$$

(b) The equipment-plate interaction is governed by

$$f\ (t) = k\ (u-w(0,t)) \tag{3-7}$$

and

$$m\ddot{u} = -\ f\ (t). \tag{3-8}$$

The appropriate regularity and force balance conditions at the plate center are

$$w\ (0,t) < \infty \tag{3-9}$$

and

$$\lim_{r \to 0} 2\pi r Q_r = -(f+P(t)) \tag{3-10}$$

where P(t) is the applied shaker force at the center of the plate.

Thus, the three possible excitations of interest are represented by

$$p(r,t) = p\, e^{i\omega t} \tag{3-11}$$

$$P(t) = P\, e^{i\omega t} \tag{3-12}$$

and $A_s \exp\left[i\,(t+x/c_s)\right]$ and in the subsequent analysis the quantities P, P, A_s and ω will be considered as specified. The acceleration of the equipment mass will be the result of interest. Since the inputs are oscillatory with specified frequency ω it is convenient to introduce the variables W, U, F, where

$$w(r,t) = W\, e^{i\omega t},\ W = W(r) \tag{3-13}$$

$$u = U\, e^{i\omega t} \tag{3-14}$$

$$f = F\, e^{i\omega t} \tag{3-15}$$

in terms of which the governing equations of the plate and the interactions are

$$D_p \nabla^4 W - \mu_p \omega^2 W = p,\ r > 0 \tag{3-16}$$

$$W_{,r}(a) = 0 \tag{3-17a}$$

$$\lim_{r \to 0} W < \infty \tag{3-17b}$$

$$\lim_{r \to 0} 2\pi r D_p (\nabla^2 W)_{,r} = F + P \tag{3-17c}$$

$$W(a) = A_s + B_s \tag{3-17d}$$

$$D_p (\nabla^2 W(a))_{,r} = \frac{i\omega}{c_s} (A_s - B_s) E_s t_s \tag{3-17e}$$

with

$$F = m\omega^2 U = k\,(U-W(0)) \tag{3-18}$$

3.2. ANALYSIS

The general solution of Equation (3-16) is

$$W(r) = A J_o(\alpha r) + B Y_o(\alpha r) + C I_o(\alpha r) + D K_o(\alpha r) - \frac{p}{\mu_p \omega^2} \quad (3\text{-}19)$$

where for simplicity we have taken $p(r) = \text{const.} = p$ and where

$$\alpha^4 = \mu_p \omega^2 / D_p. \quad (3\text{-}20)$$

In this equation A, B, C and D are constants to be determined from the boundary conditions and J_o, Y_o are Bessel's functions of zero order of the first and second kind, respectively, and I_o, K_o are modified Bessel functions of zero order. The functions $Y_o(x)$ and $K_o(x)$ exhibit singular behavior at $x = 0$ having representations near $x = 0$ of the forms

$$Y_o(x) = \frac{2}{\pi} \ln x$$

$$K_o(x) = -\ln x, \quad x \simeq 0.$$

Thus, the regularity condition (17c) requires

$$B \frac{2}{\pi} = D$$

leading to

$$W(r) = A J_o(\alpha r) + C I_o(\alpha r) + B \left(Y_o(\alpha r) + \frac{2}{\pi} K_o(\alpha r)\right) - \frac{p}{\mu_p \omega^2}.$$

Using Equation (3-1) leads to

$$\lim_{r \to 0} 2\pi r Q_r = -\lim_{r \to 0} 2\pi D_p \alpha^3 r \left(A J_1(\alpha r)\right) + C I_1(\alpha r) + B \left(Y_1(\alpha r) - \frac{2}{\pi} K_1(\alpha r)\right) \quad (3\text{-}21)$$

The functions Y_1 and K_1 exhibit singular behavior at r = 0 of the form

$$Y_1 (\alpha r) = - \frac{2}{\pi \alpha r}$$

$$K_1 (\alpha r) = \frac{1}{\alpha r}, \; r \simeq 0$$

whereas

$$J_1 (0) = 0$$

and

$$I_1 (0) = 0.$$

This Equation (3-21) leads to

$$B = - \frac{F + P}{8D_p \alpha^2}$$

and

$$W (r) = A J_o (\alpha r) + C I_o (\alpha r) - \frac{F + P}{8D_p \alpha^2} (Y_o (\alpha r) + \frac{2}{\pi} K_o (\alpha r))$$

$$- \frac{p}{\mu_p \omega^2}$$

When applied to the above equation boundary condition (3-17a) leads to

$$- A J_1 + C I_1 + \frac{F + P}{8D_p \alpha^2} (Y_1 + \frac{2}{\pi} K_1) = 0 \qquad (3\text{-}22)$$

where, above, and in what follows, the arguments of the Bessel functions are αa.

The interaction Equation (3-17d) gives

$$A J_o + C I_o \; \frac{F + P}{8D_p \alpha^2} (Y_o + \frac{2}{\pi} K_o) - \frac{p}{\mu_p \omega^2} = A_s + B_s \qquad (3\text{-}23)$$

and Equation (3-17e)

$$-D_p \alpha^3 \left[A J_1 + C I_1 - \frac{F + P}{8D_p \alpha^2} (Y_1 - \frac{2}{\pi} K_1)\right] = E_s t_s \frac{i\omega}{c_s} (A_s - B_s) \qquad (3\text{-}24)$$

Equation (3-18) provides finally

$$(-m\omega^2 + k)\ U = k\ (A + C - \frac{p}{\mu_p \omega^2}) \qquad (3\text{-}25)$$

Substitution of $m\omega^2 U$ for F in the above system of Equations (3-22 through 3-25) leads to four equations relating the four unknowns A, C, U and B_s in terms the input quantities A_s, p, P and the frequency ω. The important quantity is the absolute acceleration of the mass $|\omega^2 U|$ and is not necessary to obtain A, C and B_s. By manipulation of Equation (3-23), Equation (3-24) B_s can be eliminated obtaining

$$A\ (J_o + i\beta\ J_1) + C\ (I_o + i\beta\ I_1) -$$

$$- \frac{F + P}{8D_p \alpha^2} \left[Y_o + i\beta\ Y_1 + \frac{2}{\pi}\ (K_o - i\beta\ K_1)\right] - \frac{p}{\mu_p \omega^2} = 2\ A_s \qquad (3\text{-}26)$$

where $\beta = D_p\ \alpha^3\ c_s/\omega E_s t_s$.

Equations (3-22) and (3-25) can now be used to determine expressions for A and C in terms of U, p and P which are substituted into Equation (3-26) above to determine a single expression for U in terms of p, P and A_s. The result may be expressed in the form

$$\{N + iR\ (\frac{\omega}{\omega_*})^{1/2}\ Q\}\ U = 2\ A_s + \frac{p}{\mu_p \omega^2}\ \{S + iR\ (\frac{\omega}{\omega_*})^{1/2}\ T\}$$

$$+ \frac{P}{8D_p \alpha^2}\ \{V + iR\ (\frac{\omega}{\omega_*})^{1/2}\ Z\}$$

where

$$N = \frac{1}{J_1 + I_1}\ \{\left[J_o\ I_1 + I_o\ J_1\right]\ \left[1 - \frac{\omega^2}{\omega_o{}^2}\right]$$

$$+ \gamma\ \frac{\omega}{\omega_*}\ \left[(Y_1 + \frac{2}{\pi}\ K_1)\ (J_o - I_o)\right.$$

$$\left. - (Y_o + \frac{2}{\pi}\ K_o)\ (J_1 + I_1)\right]\}$$

$$Q = \frac{2}{J_1 + I_1} \{J_1 I_1 (1 - \frac{\omega^2}{\omega_o}_2) - \gamma \frac{\omega}{\omega_*} [I_1 Y_1 - \frac{2}{\pi} J_1 K_1]\}$$

$$S = \frac{1}{J_1 + I_1} \{J_1 + I_1 - [I_1 J_o + I_o J_1]\}$$

$$T = - \frac{2 I_1 J_1}{J_1 + I_1}$$

$$V = \frac{1}{J_1 + I_1} \{[Y_o + \frac{2}{\pi} K_o] [J_1 + I_1] - [Y_1 + \frac{2}{\pi} K_1] [J_o - I_o]\}$$

$$Z = \frac{2}{J_1 + I_1} \{I_1 Y_1 - \frac{2}{\pi} J_1 K_1\}$$

where the arguments of the Bessel's functions are $\alpha a = (\frac{\omega}{\omega_*})^{1/2}$.

The parameters, R, γ and ω_* are independent of ω and represent a reflection coefficient, a mass ratio and a characteristic frequency of the plate, respectively. They are defined by

$$R = \frac{\rho_p c_p t_p}{\rho_s c_s t_s}$$

$$\gamma = \frac{m}{8\mu_p a^2}$$

$$\omega_* = (D_p/\mu_p)^{1/2}/a^2$$

It is to be noted that ω_* is not the fundamental frequency of the plate but that the natural frequencies of the plate itself can be expressed in terms of ω_*. The quantity c_p is a fictitious plate speed defined by $c_p = a\omega_*$.

3.3. RESULTS AND NUMERICAL EXAMPLES

It is convenient at this point to give the results for the three input cases separately. The amplification factor for the case of ground shock is taken as $|U/A_s|$ since this represents both the ratio of displacements and the ratio of the equipment acceleration to the ground shock acceleration. In the other two cases the amplification factor should involve the equipment acceleration and the force terms and these are of different dimension. The results are:

a. Ground Shock Input

$$\left|\frac{U}{A_s}\right| = \frac{2}{\left[N^2 + R^2 \left(\frac{\omega}{\omega_*}\right) Q^2\right]^{1/2}} \tag{3-27}$$

b. Air Shock Input

$$\left|\frac{\omega^2 \, U/t_p}{\omega_*^2 \, \tilde{p}}\right| = \frac{\left\{\left[SN + R^2 \left(\frac{\omega}{\omega_*}\right) TQ\right]^2 + R^2 \left(\frac{\omega}{\omega_*}\right) \left[SQ - TN\right]^2\right\}^{1/2}}{N^2 + R^2 \left(\frac{\omega}{\omega_*}\right) Q^2} \tag{3-28}$$

where

$\tilde{p} = \dfrac{p}{\mu_p t_p \omega_*^2}$ is a dimensionless pressure.

c. Shaker Input

$$\left|\frac{\omega^2 \, U/a}{\omega_*^2 \, \tilde{P}}\right| = \frac{\omega}{\omega_*} \frac{\left\{\left[VN + R^2 \left(\frac{\omega}{\omega_*}\right) ZQ\right]^2 + R^2 \left(\frac{\omega}{\omega_*}\right) \left[VQ - ZN\right]^2\right\}^{1/2}}{N^2 + R^2 \left(\frac{\omega}{\omega_*}\right) Q^2} \tag{3-29}$$

where

$P = \dfrac{\tilde{P}a}{8D_p}$ is a dimensionless force.

The parameter R expresses the reflection-transmission characteristics of the interface between the plate and the shell. When a pulse travels up the shell to the interface some energy is reflected back into the shell and some is

transmitted into the plate. If R is less than 1 the reflected wave is an unloading pulse and R greater than 1 means that a loading wave is reflected back into the shell. The coefficient depends on the relative dynamic stiffness of the two elements and in this case it seems likely that the plate being a flexural element will be much less stiff than the shell.

The existence of radiation damping in the system is due to finite values of R; as $R \to 0$ the shell becomes infinitely stiff and the equations reduce to those of a clamped plate, and as $R \to \infty$ to those of a free plate (with edges prevented from rotating). When $R \to 0$ each of the three solutions reduces to terms having only N as the denominator. The amplification factors thus tend to infinity at the zeroes of N. In the case $\gamma = 0$ the zeroes of N are given by

$$J_o\left(\sqrt{\omega/\omega_*}\right) I_1\left(\sqrt{\omega/\omega_*}\right) + I_o\left(\sqrt{\omega/\omega_*}\right) J_1\left(\sqrt{\omega/\omega_*}\right) = 0 \qquad (3\text{-}30)$$

which is the characteristic equation for the natural frequencies of a clamped plate. The roots of this equation are tabulated in Jahnke and Emde (Reference 13). When $R \to \infty$ each of the three solutions reduce to expressions with Q as the denominator and for $\gamma \to 0$ the zeroes of Q are given by

$$J_1\left(\sqrt{\omega/\omega_*}\right) I_1\left(\sqrt{\omega/\omega_*}\right) = 0$$

which is recognized as the equation for the natural frequencies of a free plate with edges constrained against rotation.

Based on the dimensions of a typical silo, cases have been considered where R = 0.01, 0.05 and γ = 0.01, .001, .001 and Equation (3-27) and have been computed. The results for the air shock turn out to be very similar to the ground shock case and have not been included. In these examples it has been assumed that the equipment is tuned to the fourth natural frequency of the plate. Typical results are shown in Figures 8 and 9.

It is clear that the results for both cases are qualitatively similar to the earlier results on the more simplified model. To gain insight into the origin of the double peak for this more complex system some of the asymptotic properties of the Bessel functions may be utilized since the value of (ω/ω_*) near the double root is large.

For small R the amplification peaks are given by the zeroes of N, namely by those values of ω satisfying

$$\left[J_o\, I_1 + I_o\, J_1\right]\left[1 - \frac{\omega^2}{\omega_o{}^2}\right] = \gamma\,\frac{\omega}{\omega_*}\left\{\left[Y_o + \frac{2}{\pi}\,K_o\right]\left[J_1 + I_1\right]\right.$$

$$\left. - \left[Y_1 + \frac{2}{\pi}\,K_1\right]\left[J_o - I_o\right]\right\}. \qquad (3\text{-}31)$$

For large values of the argument of the Bessel functions, namely $\sqrt{\omega/\omega_*}$ (here $\omega_o = (12.58)^2\,\omega_*$, 12.58 being the fourth root of the eigenvalue equation), the Bessel functions can be approximated by asymptotic expansions. These are:

$$J_o\,(x) = \sqrt{\frac{2}{\pi x}}\left\{\cos\,(x - \frac{\pi}{4}) + \frac{1}{8x}\,\sin\,(x - \frac{\pi}{4})\right\}$$

$$Y_o\,(x) = \sqrt{\frac{2}{\pi x}}\left\{\sin\,(x - \frac{\pi}{4}) - \frac{1}{8x}\,\cos\,(x - \frac{\pi}{4})\right\}$$

$$J_1\,(x) = \sqrt{\frac{2}{\pi x}}\left\{\cos\,(x - \frac{3\pi}{4}) - \frac{3}{8x}\,\sin\,(x - \frac{3\pi}{4})\right\}$$

$$Y_1\,(x) = \sqrt{\frac{2}{\pi x}}\left\{\sin\,(x - \frac{3\pi}{4}) + \frac{3}{8x}\,\cos\,(x - \frac{3\pi}{4})\right\}$$

$$I_o\,(x) = \frac{e^x}{\sqrt{2\pi x}}$$

$$I_1\,(s) = \frac{e^x}{\sqrt{2\pi x}}$$

$$K_o\,(x) = e^{-x}\sqrt{\frac{\pi}{2x}}$$

$$K_1\,(x) = e^{-x}\sqrt{\frac{\pi}{2x}}$$

After substituting these asymptotic forms into Equation (3-31) and considerable manipulation, the equation takes the form

$$\sin\,(\sqrt{\omega/\omega_*})\left[1 - \frac{\omega^2}{\omega_o{}^2}\right] = -\,\gamma\,\frac{\omega}{\omega_*}\,\cos\,(\sqrt{\omega/\omega_*})$$

This expression may be expected to be highly accurate for all values of the argument larger than the lowest frequency of the plate and even in that case the accuracy is quite good, e.g., the first root of the exact expression (Equation 3-30) is 3.2 while the asymptotic expansion of it gives 3.14.

The roots of the above equation are given by

$$\frac{\tan\left(\sqrt{\omega/\omega_*}\right)}{\omega/\omega_*} = \frac{-\gamma}{1 - \omega^2/\omega_o{}^2} \quad .$$

Figure 10 shows

$$\frac{\tan\left(\sqrt{\omega/\omega_*}\right)}{\omega/\omega_*}$$

and $\frac{-\gamma}{1 - \omega^2/\omega_o{}^2}$ for the case where the equipment frequency ω_o is tuned to a natural frequency of the plate. When this is a high mode the term (ω/ω_*) in the denominator is very large and tends to flatten the tangent curve. For fixed nonzero γ the roots in the high frequency case tend to be located at values of $(\omega/\omega_*)^{1/2}$ which are $\pm\ \pi/2$ distance from the particular natural frequency of the plate to which the equipment is tuned. For low frequency cases, however, the roots tend to coalesce as γ becomes small. There are two approximations. In the low frequency case the spread between the peaks of the double resonance is given by

$$\frac{\Delta\omega}{\omega_o} = 2\sqrt{\lambda_n \gamma}$$

and for high frequency cases

$$\frac{\Delta\omega}{\omega_o} = \frac{2}{n}$$

where n is the mode number of the plate natural frequency and λ_n is the nth root of Equation (3-30) which is related to the frequency of the nth plate mode ω_n through

$$\omega_n = \lambda_n{}^2\ \omega_* .$$

These results indicate the spread between the double peaks increases as the equipment is tuned to higher plate frequencies for low order modes and subsequently decreases for higher order modes. The phenomenon of the double peak is thus an intermediate frequency one, possibly not as important in either the low range or the very high range, since the existence of the double peak provides a range of frequency over which the system is susceptible to resonant conditions.

Numerical computations of the amplification factor given in Equation (3-29) are shown in the sequence Figures 11a through 11e in which results for shaker excitation are shown when the equipment is tuned to the first five natural frequencies of the plate in turn. In these diagrams the frequency is scaled in such a way that the equipment frequency is unity so that there is a compression of the frequency scale; in terms of real frequency the increased spread in the double peak is clear.

Figure 12 shows how the spread varies with mode number of the support. The spread is greatest, offering the greatest target for resonance, at an intermediate frequency; for the parameters of the system shown in Figure 12, the fourth mode offers the largest target. Figure 13 shows how the amplification of the equipment at resonance varies with mode number of the support. Both Figures 12 and 13 indicate that the double resonance phenomenon is critical at intermediate frequencies. Figure 13 shows that, for the parameters considered, the equipment acceleration can be as much as 5,000 times greater than the input acceleration. The results in these figures include only the effects of radiation-type damping (energy radiated into the supporting structure) and will be reduced (probably significantly) when structural damping is introduced.

SECTION 4

ALTERNATIVE MODELS OF DAMPING FOR HIGH FREQUENCY ANALYSIS

4.1. MAXWELL MODEL OF DAMPING

An alternative simple modeling of structural damping which has the same degree of simplicity as the usual damping model, but which it is believed will lead to an improved estimate of structural response at high frequencies is introduced. The model is based on the well known Maxwell model of viscoelasticity and thus, in a one degree-of-freedom system, requires only one damping parameter.

It is known from analyses of wave propagation in viscoelastic materials that given the appropriate type of viscoelastic model a continuum can propagate discontinuities as waves. The essential requirement is some form of instantaneous elasticity in the model. The material will also be dissipative and the discontinuity may be attenuated as it propagates through the material, but the presence of dissipation by itself is not a counter to the existence of a discontinuity. There are models of material behavior, for example the Navier-Stokes theory for fluids and the Kelvin-Voigt theory for solids, which do not permit the existence of discontinuities. In both these models there can be no acceleration waves and essentially this result arises from the lack of an instantaneous elastic response in these models.

The notions of instantaneous response and acceleration waves in extended continua are very closely related to high frequency behavior in bounded systems, and thus it is obvious that much the same considerations will pertain to these situations.

In structural dynamics damping is generally included in the structural model in the form of viscous damping or the modification of it which is referred to as structural or hysteretic damping. The viscous damping structural model is an analogue of the Kelvin-Voight viscoelastic continuum model, and thus it seems clear that high frequency response and short time response would be better modeled by the use of a structural model

which is analogous to the Maxwell viscoelastic continuum model. Such a model is developed in the following section and it is shown that it needs no more information to specify it than does the usual viscous damping model and that many of the characteristics of viscous damping carry over to the new model.

Although it is relatively straight forward to specify the elastic and inertial characteristics of a structural system it is very much more difficult to specify the damping characteristics. Normally a rule of thumb approximation is used in which the damping in each model is assigned. Exactly the same form can be used in this approach.

4.2. GOVERNING EQUATIONS OF MAXWELL MODEL

The most effective way to illustrate the behavior of the damping model suggested here is to study the response of a single degree-of-freedom system. In this case, the equation of motion is governed by

$$m\ddot{u} + F = P(t) \tag{4-1}$$

with

$$\frac{\dot{F}}{F_o} = \frac{\dot{u}}{u_o} - \frac{1}{t}\left(\frac{F}{F_o}\right) \tag{4-2}$$

To express these equations in non-dimensional variables, define

$$\omega_o^2 = mu_o/F_o, \quad T = 2\pi/\omega_o$$

$$\xi = 1/2\tau\omega_o$$

$$x = \omega_o t$$

$$y = u/u_o$$

$$f = F/F_o$$

then

$$y'' + f = p(x) \tag{4-3}$$

$$f' = y' - 2\xi f \tag{4-4}$$

where $p(x) = P(t)/F_o$, and primes denote differentiation with respect to x.

For the first example, steady-state response under sinusoidal loading, i.e., $P(t) = P_o \sin\omega t$ or $p(x) = R \sin\beta x$, $R = {}^{P_o}/_{F_o}$, is $\beta = \omega/\omega_o$ investigated. By eliminating f from Equation (4.3)

$$y'''' + 2\xi y'' + y' = R\,(2\xi \sin\beta x + \beta \cos\beta x)$$

and the steady-state amplitude $\bar{y}$ is then given by

$$\bar{y} = R\,\frac{1}{\beta^2}\,\frac{\sqrt{\beta^4(1-\beta^2)^2 + (2\xi\beta)^2\,(1+2\beta^2-2\beta^4) + (2\xi\beta)^4}}{(1-\beta^2)^2 + (2\xi\beta)^2}$$

for $\xi = 0$, the amplitude for an undamped system is recovered,

$$\bar{y} = \frac{R}{(1-\beta^2)}$$

Moreover, for the undamped case,

$$\lim_{\beta\to 0} \bar{y} = R$$

i.e., as the frequency of the load approaches zero, the displacement is bounded and approaches

$$u_o = \frac{P_o}{K_o}$$

$$K_o = \frac{F_o}{u_o}$$

For ξ different from zero, however $\bar{y}$ grows without bound as $\beta\to 0$. This is indeed expected, since the Maxwell model behaves like a fluid under small displacement rates. Figure 14 shows a plot of $\bar{y}/R$ versus β where this is clearly exhibited.

4.3. GENERALIZATION TO MULTI DEGREE-OF-FREEDOM SYSTEMS

In view of the fact that the most common method of introducing damping in structural dynamics problems is to resort to the Kelvin model of linear viscoelasticity, a comparison of Kelvin and Maxwell models is in order. Consider the dynamic equations of equilibrium for a multi degree-of-freedom system:

$$\underset{\sim}{M}\,\ddot{\underset{\sim}{u}} + \underset{\sim}{F} = \underset{\sim}{P}$$

with

$$\dot{\underset{\sim}{F}} = \underset{\sim}{K}\,\dot{\underset{\sim}{u}} - \underset{\sim}{C}^{*}\,\underset{\sim}{F}$$

These two equations lead to the third order linear differential equation

$$\underset{\sim}{M}\,\ddot{\underset{\sim}{u}} + \underset{\sim}{C}^{*}\,\underset{\sim}{M}\,\ddot{\underset{\sim}{u}} + \underset{\sim}{K}\,\dot{\underset{\sim}{u}} = \underset{\sim}{C}^{*}\underset{\sim}{P} + \dot{\underset{\sim}{P}} \qquad (4\text{-}5)$$

Let $\underset{\sim}{C} = \underset{\sim}{C}^{*}\,\underset{\sim}{M}$ and integrate Equation (4-5) to obtain

$$\underset{\sim}{M}\,\ddot{\underset{\sim}{u}} + \underset{\sim}{C}\,\dot{\underset{\sim}{u}} + \underset{\sim}{K}\,\underset{\sim}{u} =$$

$$\underset{\sim}{P} + \left\{\int_{o}^{t} \underset{\sim}{C}\,\underset{\sim}{M}^{-1}\,\underset{\sim}{P}\,dt + \left[\underset{\sim}{C}\,\dot{\underset{\sim}{u}} + \underset{\sim}{K}\,\underset{\sim}{u} - \underset{\sim}{F}\right]_{t\,=\,0}\right\}$$

On the other hand, assuming that the internal forces are governed by a Kelvin model, i.e.,

$$\underset{\sim}{F} = \underset{\sim}{K}\,\underset{\sim}{u} + \underset{\sim}{C}\,\dot{\underset{\sim}{u}}$$

the displacement equations of equilibrium take the form:

$$\underset{\sim}{M}\,\ddot{\underset{\sim}{u}} + \underset{\sim}{C}\,\dot{\underset{\sim}{u}} + \underset{\sim}{K}\,\underset{\sim}{u} = \underset{\sim}{P} \qquad (4\text{-}6)$$

Thus, both the Kelvin and Maxwell models lead to the same differential equation, but have different forcing functions. This implies that a computer program designed for solving Kelvin-type problems can be easily modified to solve systems with Maxwell-type damping. In fact, this can be accomplished even in the pre-processing stage of computing the loads for a system.

A significant difference exists between Equation (4-5) and Equation (4-6) in initial conditions that need to be specified. Equation (4-6) requires that the displacement $\underset{\sim}{u}_{o}$ and velocity $\dot{\underset{\sim}{u}}_{o}$ at time t_{o} be known to obtain the solution; these quantities completely determine the force F at t_{o} via

$$\underset{\sim}{F} = \underset{\sim}{K}\,\underset{\sim o}{u} + \underset{\sim}{C}\,\dot{\underset{\sim o}{u}}$$

With a Maxwell model, however, these quantities do not determine the initial value of $\underset{\sim}{F}$; in fact, the value of F at t_{o} must be specified in addition to

$\underset{\sim}{u}_o$ and $\dot{\underset{\sim}{u}}_o$. This aspect of the Maxwell model suggests that it might indeed be more suitable than the Kelvin model for impact problems. For, while a structural system at rest acquires an initial velocity following an impact, it is not reasonable to assume that this also results in non-zero values for resisting forces. The use of a Kelvin model does incorporate such an assumption, and, if the damping matrix $\underset{\sim}{C}$ is proportional to the stiffness, $\underset{\sim}{K}$ it leads to high accelerations and low displacements in the higher modes. In contrast, the Maxwell model results in more flexible response and gives lower accelerations and higher displacements. With mass proportional damping, modal damping is inversely proportional to modal frequency and both models give essentially the same answers for the low damping ratios resulting from such an assumption. Of course, many of the difficulties attendant on the use of viscous damping in structural analysis of impact problems or high frequency analysis could be alleviated by the use of general viscoelastic models to represent the response of the system. However the degree of complication which results would be considerable for a large system and it would be almost impractical to obtain the necessary experimental data to define the response. What is needed is some model which has the simplicity of the viscous model which can be generally defined simply by specifying a damping factor for each mode.

It seems likely that the Maxwell model when converted to the structural problem might be useful for high frequency analysis. It should be noted that the same number of parameters are needed to define the Maxwell model as are needed for the Kelvin model and that the use of modal damping factors would also suffice.

SECTION 5

APPLICATION OF RESULTS TO E.D.C. TEST

This theory can be applied to the forthcoming series of tests on the Electrical Distribution Center (EDC) to be conducted for DNA during the Summer of 1977. The equipment, part of the safeguard system, in this system is carried on a rectangular plate suspended by four shock isolation devices. Thus the system is close to the theoretical model considered in Section 3 of this report and it is possible that some items of equipment carried on the isolated plate may in fact be tuned to some natural frequency of the system. Shaker excitation applied to the roof of the building will correspond to the ground shock solution and shaker excitation applied to the plate will correspond to the shaker excitation problem. Acceleration measurements on various items of equipment on the isolation system under these two types of excitation would be useful and revealing.

The main difficulty in making quantitative predictions of the response of the EDC during the testing program is of course the lack of detailed information on the building, on the platform and on the isolators themselves. Some information has been provided by Waterways Experiment Station (WES), Vicksburg, who is conducting the tests on the building and platform which has enabled estimates to be made of the platform loading and its bending stiffness. On the basis of this data the platform has been modeled as an isotropic plate with an effective moment of inertia of 100 in.^{4} per inch. The weight of the electrical equipment carried by the platform, reported by WES as 60,000 pounds, was assumed to be uniformly distributed resulting in a plate mass per unit area (including the self weight) of 0.75 pounds per square inch.

Information from Barry Burbank, the manufacturers of the isolators (References 14 and 15) suggests that an isolator can be considered as a spring which when carrying a mass of 20,000 pounds gives a frequency of 0.73H. This leads to a spring stiffness k given by

$$k = m\omega^2$$

of 1,100 pounds/inch for each isolator.

The platform plan dimensions are very nearly square with average side length 25 feet. The fundamental mode of a completely free square plate is one in which there are nodal lines through the center of the plate parallel to the sides. The exact solution for this case is not known but an approximation to the frequency can be obtained using Rayleigh's principle assuming a mode shape of the form $w = xy$. In the particular problem considered herein the same mode shape is maintained and the contribution of the isolators to the potential energy is included. Assuming a steady harmonic motion of the form $w = 4w_o/a^2\ xy \cos \omega t$, the strain energy stored in the plate is

$$V_p = \frac{32E\ h^3\ w_o^2}{3(1+\nu)\ a^2} \cos^2 \omega t$$

where E is Young's modulus, h is the half thickness, a is the length of the edge, ν is Poisson's ratio and ω is the circular frequency of oscillation. For the parameter values utilized here this yields $V_p = 4 \times 10^5 w_o^2$ pounds per inch, where E has been taken to be 30×10^6 psi and $\nu = 1/3$. The total potential energy stored in the four isolators is given by

$$V_I = 4 \cdot \frac{1}{2} k\ w_o^2 \cos^2 \omega t$$

which results in $V_I = 2{,}200\ w_o^2$ pounds per inch. Thus the total potential energy of this subsystem is $402{,}000\ w_o^2$ pounds per inch. The kinetic energy of the plate is

$$T = \frac{1}{9} \rho\ h\ a^4\ w_o^2\ \omega^2 \sin^2 \omega t$$

where ρ is the mass per unit of volume. Applying Rayleigh's principle, the fundamental frequency is estimated as 23 Hz.

The next highest natural frequency is one in which the diagonals of the plate are nodal lines. Rayleigh (Reference 16) estimates that this

frequency will be about 30 percent higher than the fundamental one, resulting in a figure of 30 Hz.

These calculations indicate that the double peak amplification phenomenon could show up in the response of the platform in the frequency range 20 Hz to 35 Hz. The frequency spread at a double peak dictates the shifting down of the frequency range lower limit and shifting up of the upper limit. It is difficult to estimate the spread since the effective mass of the entire structure is not known. The actual mass of the entire structure exceeds 1,200,000 pounds but the contribution from backfill is not known. The total mass of the platform is around 70,000 pounds indicating a mass ratio around 0.06. For such a mass ratio the spread is about 20 percent of the central frequency.

From information provided by WES the structure itself appears to have a number of resonances below, in and above this range and thus if one of the structural frequencies is close to one of the platform frequencies the double peak should appear in the response of the platform.

It is therefore recommended that the test series be planned in such a way that this phenomenon can be observed if it should occur. Acclerometers should be placed on the platform at each corner and at the center. Accelerometers should also be located at various points on the building. The shaker should be located on the building roof. The results of excitation in the frequency range 15 Hz to 45 Hz within which several building resonances are expected will be of primary interest. In particular in the range 20 Hz to 35 Hz the possibility of double peak amplification due to tuning is anticipated. If tuning occurs it is expected that the spread between peaks would be of the order of 5 Hz.

Experimental results of dynamic tests on the isolators by the manufacturers (Reference 17) suggest that the isolators are subject to a subsystem resonance at around 50 Hz and thus might be expected to interact with a platform resonance around this value if such should occur. The actual magnitude

of this internal resonance will depend on the pendant length and fixity conditions and may vary from situation to situation.

There are disadvantages in restricting attention to these measurements alone since the vibrational characteristics of the shock-isolated platform of the isolators or of the attached equipment are not accurately known. To reveal the existence of the phenomenon postulated in this report it would be necessary to add a small structure-equipment system to the platform which would undergo motions during the experiment. The properties of each element of this system would be known much more accurately than those of the existing utility and electronic substations. The new equipment element could be adjusted to be both non-tuned and tuned to several platform frequencies. For this purpose, a simple and inexpensive mounting would be adequate. A flat plate square in plan supported on four angles at the corners is suggested. On this plate to simulate equipment would be a set of reed gages of a variety of tuned and non-tuned systems. Alternatively, a small number of specially designed spring-mass oscillators with accelerometers may be used.

The results sought in these tests would be the determination of whether the double peak resonance occurs and if so at the frequencies predicted.

SECTION 6

FUTURE RESEARCH DIRECTIONS

The results described in this report suggest certain directions for future research in the analysis of equipment-structure systems at high frequency. This work falls into four main areas with substantial interaction between them.

6.1. DAMPING

The theory developed so far should be extended to include structural damping which is expected to play an important role in the response of the system. Previous work has shown that conventional structural damping models are not realistic at high frequencies and a new approach to damping suitable for high frequencies should be developed.

6.2. MULTI-MODE RESPONSE OF ATTACHED EQUIPMENT

In the previous work the equipment element of the structure-equipment system has been modeled as a single degree-of-freedom system. This should be expanded to models which include multiple degree-of-freedom behavior in the attachment. This may reveal important coupling phenomena overlooked in the simple model.

6.3. EXTENSION TO GENERAL STRUCTURAL SYSTEM

It has become clear in the course of the previous work on the idealized systems that many of the results are not special to these models, but will appear in any structural system. It should be possible to develop these results for more general structural systems utilizing a technique of cascading impedance functions for subsystems. These impedance functions may be obtained either by experiment or by suitable numerical analysis. Such information could serve as input to models of the kind used here to provide the response of real structure-equipment systems.

6.4. TRANSIENT RESPONSE

Previous work has been concerned with steady state response. Techniques needed to synthesize these results for application to transient loading typical of air shock or ground shock should be studied.

The scope of the work outlined above is broad. It must be completed before work can begin in adapting finite element techniques to high frequency problems. However, a preliminary study of integration algorithms which may be useful in treating this class of problems should be initiated. If the work described above goes smoothly, some experimentation with an existing finite element code would be appropriate.

REFERENCES

1. Houbolt, J. C., "A Recurrence Matrix Solution for the Dynamic Response of Elastic Aircraft," J. Aeronaut. Sci. 17, pp. 540-550 (1950).

2. Bathe, K. J., and Wilson, E. L., "Stability and Accuracy Analysis of Direct Integration Methods," Earthq. Eng. Str. Dyn. 1, pp. 283-291 (1973).

3. Goudreau, G. L., and Taylor, R. L., "Evaluation of Numerical Methods in Elastodynamics," J. Comp. Meth. Appl. Mech. Eng., pp. 69-97 (1973).

4. Belytschko, T., Holmes, N., and Mullen, R., "Explicit Integration--Stability Solution Properties, Cost," in Finite Element Analysis of Transient Nonlinear Structural Behavior, edited by T. Belytschko, J. R. Isias, P. V. Marcal, published by ASME, New York, 1976.

5. Chin, R. C. Y., "Dispension and Gibbs Phenomenon Associated with Difference Approximations to Initial Boundary-Value Problems for Hyperbolic Equations," UCRL-76018, Lawrence Livermore Laboratory, University of California (1974).

6. Hilber, H. M., Hughes, T. J. R., and Taylor, R. L., "Improved Numerical Dissipation for Time Integration Algorithms in Structural Dynamics," Lawrence Berkeley Laboratory, University of California, LBL-4486 (1976).

7. Hurty, W. C., and Rubinstein, M. F., "Dynamics of Structures," Prentice-Hall, Chapter 7 (1965).

8. Rosenblueth, E., and Herrera, I., "On a Kind of Hysteretic Damping," J. Eng. Mech. Div., ASCE, Vol. 90, No. EM4, pp. 37-48 (1964).

9. Geers, T. L., and DeRuntz, J. A., Lockheed Missiles and Space Company Report, LMSC-D313297, December 1972.

10. Scavuzzo, R. J., Bulletin of Seismological Society of America, Vol. 57, pp. 735-746 (1967).

11. Newmark, N. M., and Hall, W. J., "Procedures and Criteria for Earthquake Resistant Design," U. S. National Bureau of Standards, Building Science Series 46, Vol. 1, February 1973.

12. Clough, R. W., and Penzien, J., Dynamics of Structures, McGraw-Hill, p. 596 (1975).

13. Jahnke, E., and Emde, F., Table of Functions, Fourth Edition, Dover Publications, New York, 1945.

14. Steiner, E., Qualification Task Report for Pneumatic Isolators, Barry Part Nos. 92094-1 through 92094-10. Report No. WE 92094-001, Submitted to Corps of Engineers, Huntsville, Alabama, by Barry Wright Corp., Burbank, California, July 1971, Reon, A., March 1973.

15. Fox, G. L., and Steiner, E., "Transient Response of Passive Pneumatic Isolators," Shock and Vibration Bulletin, Bulletin 42, pp. 85-91, 1972.

16. Lord Rayleigh, Theory of Sound, Vol. 1, p. 379, Dover, 1945.

17. Fox, G. L., "Transient Response of Passive Pneumatic Isolators," Barry Wright Corp. Internal Report, May 1971.

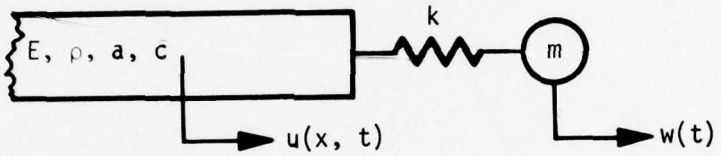

Figure 1. Diagrammatic Representation of Elementary Model

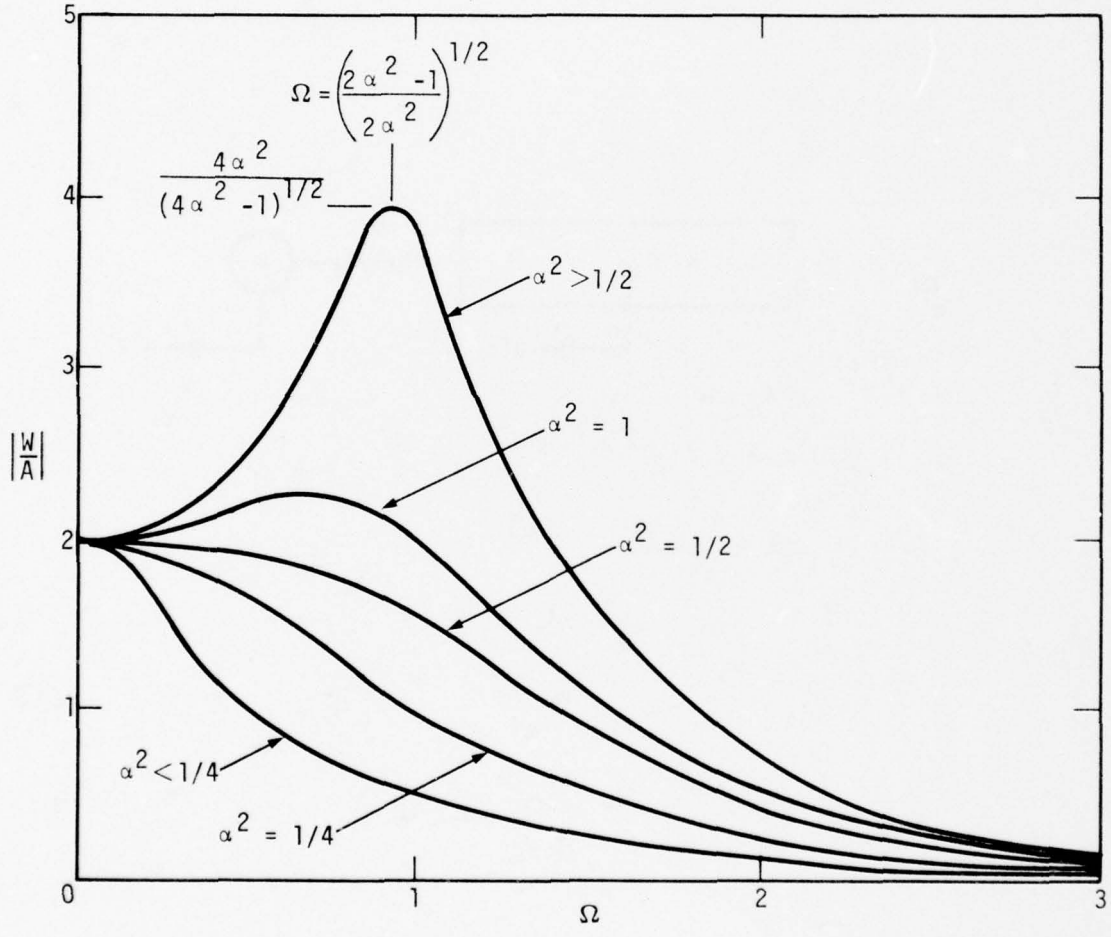

Figure 2. Amplification Factor for Elementary Model as a Function of Non-Dimensional Frequency

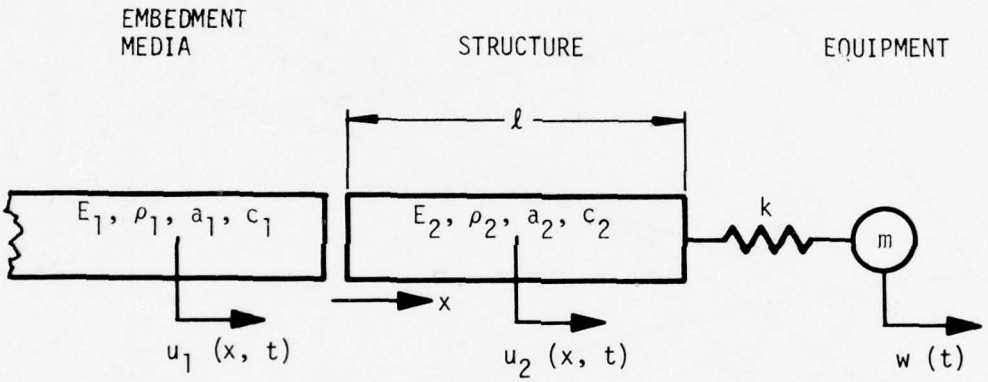

Figure 3. Diagrammatic Representation of Advanced Model

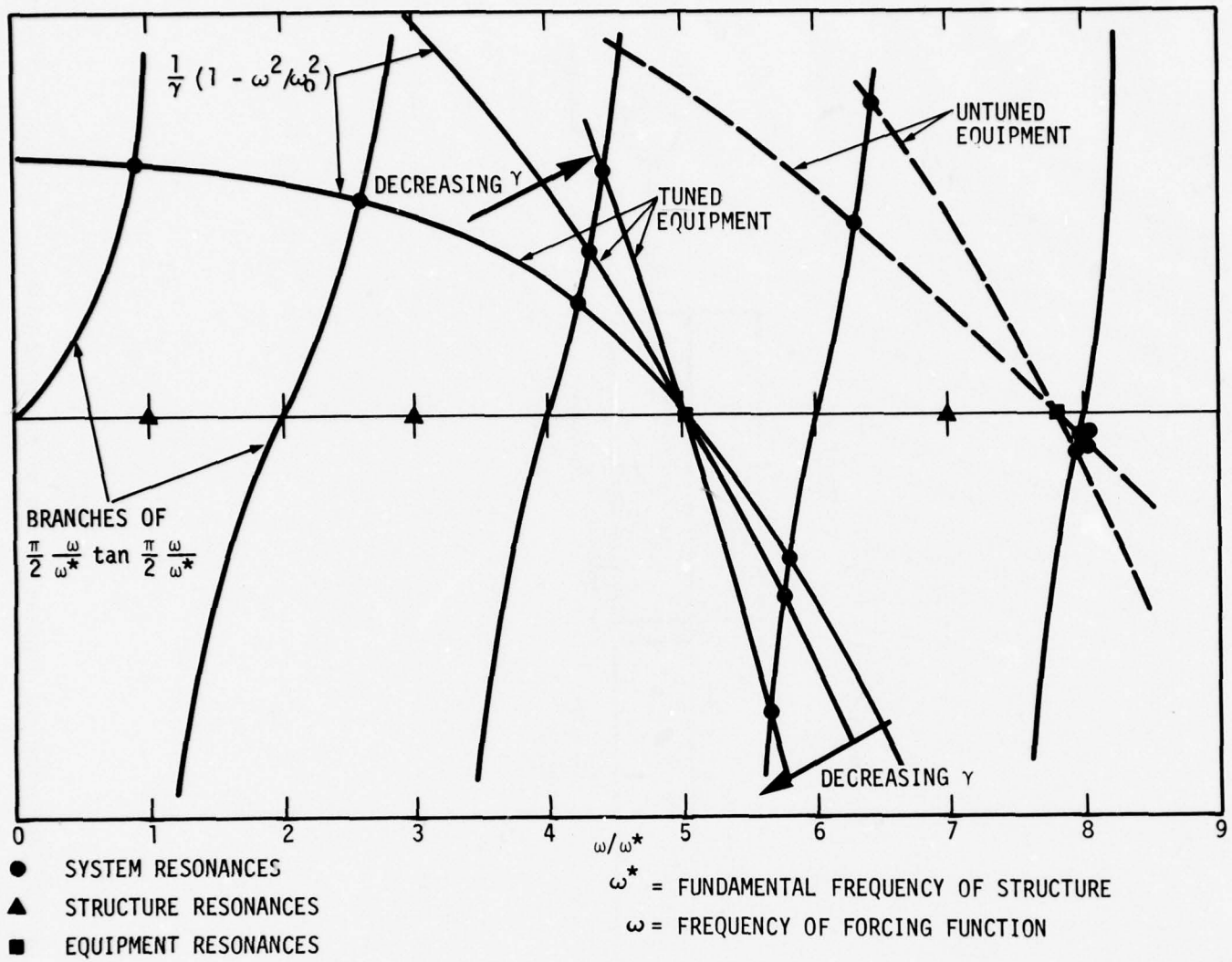

Figure 4. Solution Curves for Resonances in Advanced Model

R = ratio of $\frac{\text{soil impedance}}{\text{structure impedance}} = 0.1$

γ = mass ratio = 1/20

Ω_o = fixed base frequency of equipment = 5.0

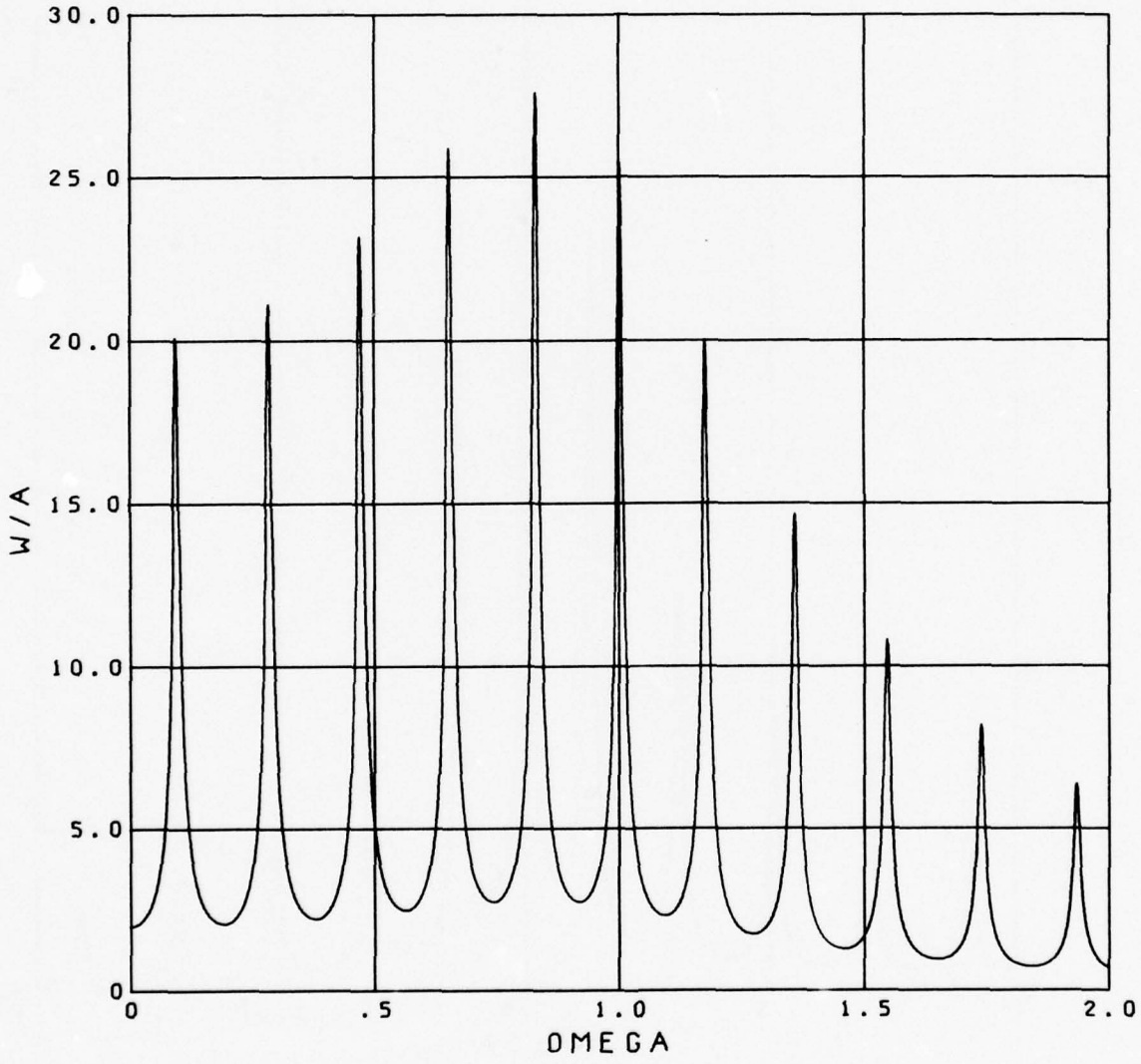

Figure 5a. Amplification Factor $\left(\frac{\text{Equipment Acceleration}}{\text{Ground Shock Acceleration}}\right)$ versus non-dimensional frequency for Untuned System (Mass Ratio 1/20)

R = ratio of $\frac{\text{soil impedance}}{\text{structure impedance}} = 0.1$

γ = mass ratio = .01

Ω_o = fixed base frequency of equipment = 5

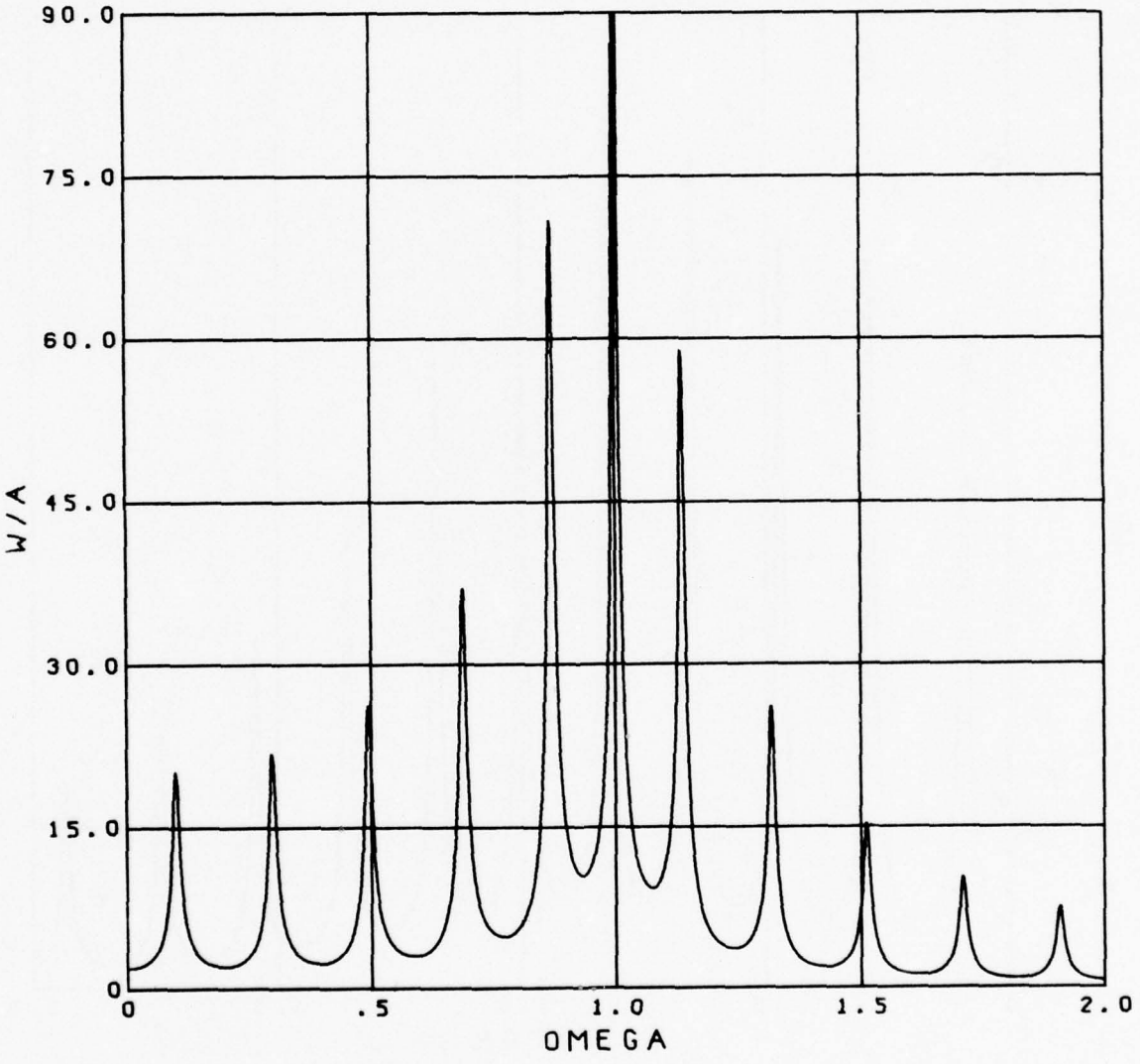

Figure 5b. Amplification Factor $\left(\frac{\text{Equipment Acceleration}}{\text{Ground Shock Acceleration}}\right)$ versus non-dimensional frequency for Untuned System (Mass Ratio 1/100)

R = ratio of $\frac{\text{soil impedance}}{\text{structure impedance}} = 0.1$

γ = mass ratio

Ω_o = fixed base frequency of equipment = 4.5

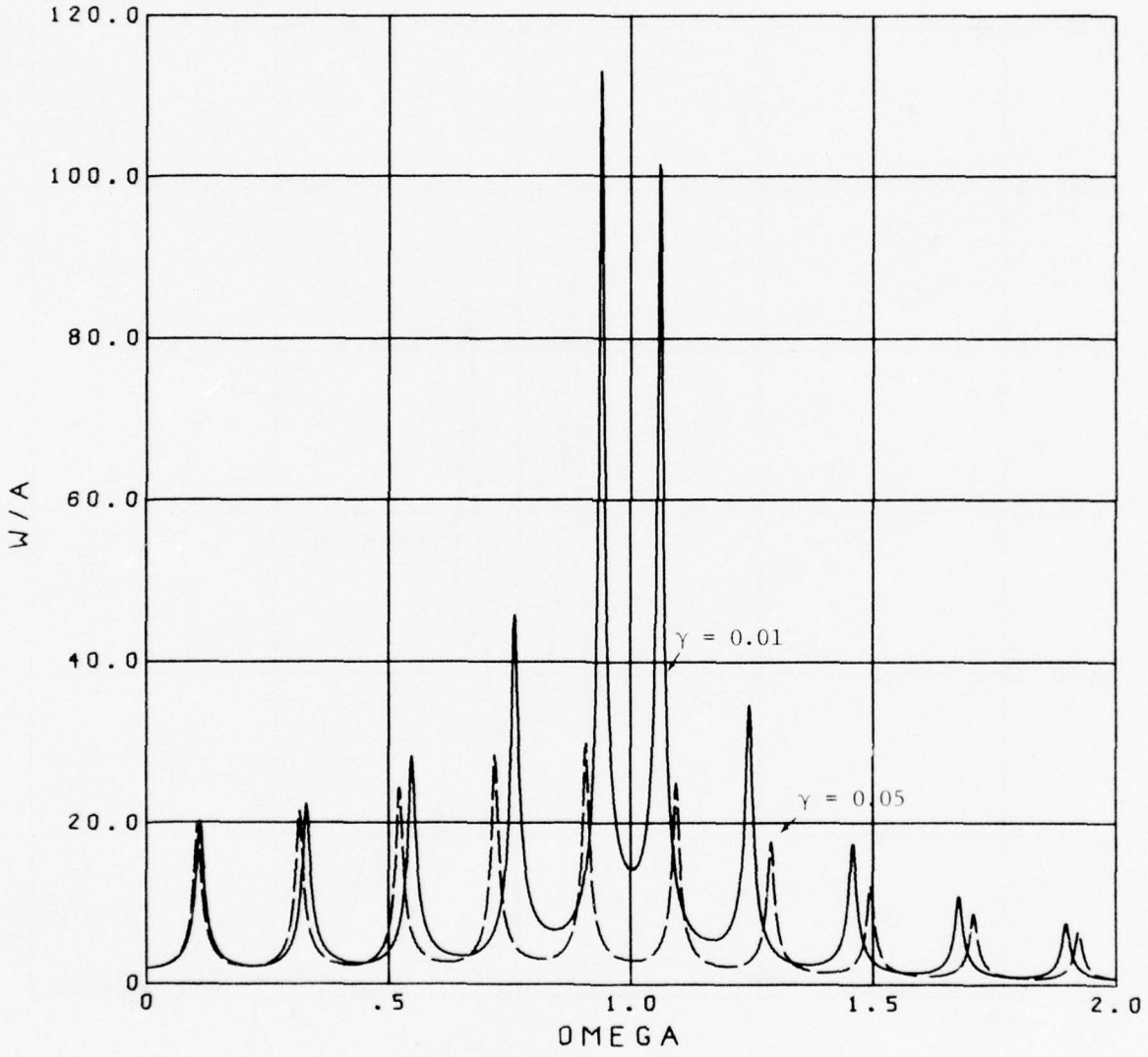

Figure 6a. Amplification Factor $\left(\frac{\text{Equipment Acceleration}}{\text{Ground Shock Acceleration}}\right)$ versus non-dimensional frequency for Tuned System

R = *ratio of* $\frac{\text{soil impedance}}{\text{structure impedance}} = 0.1$

γ = mass ratio

Ω_o = fixed base frequency of equipment ≈ 4.5

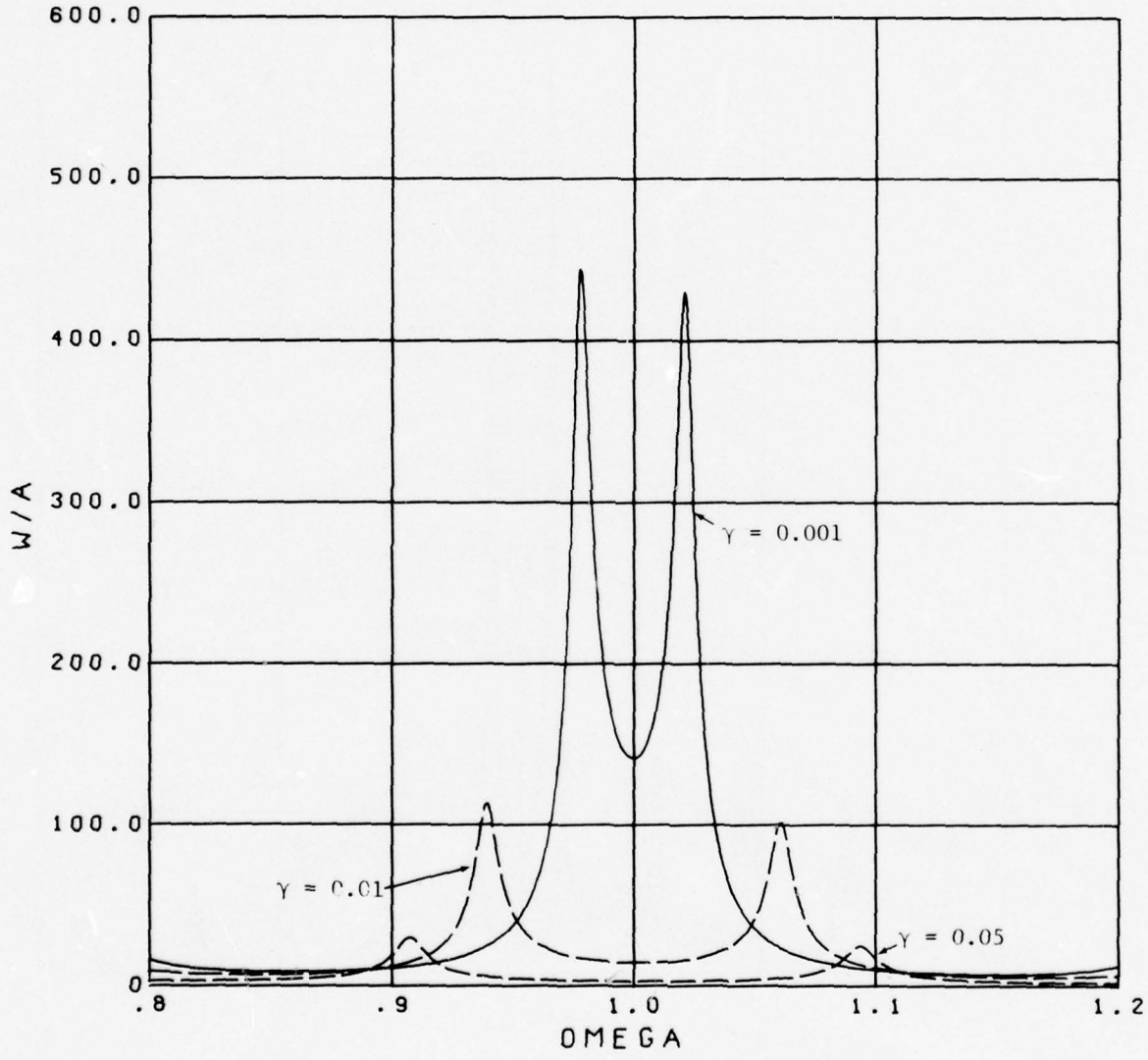

Figure 6b. Same as Figure 6(a) with Expanded Scale Near Equipment Resonance

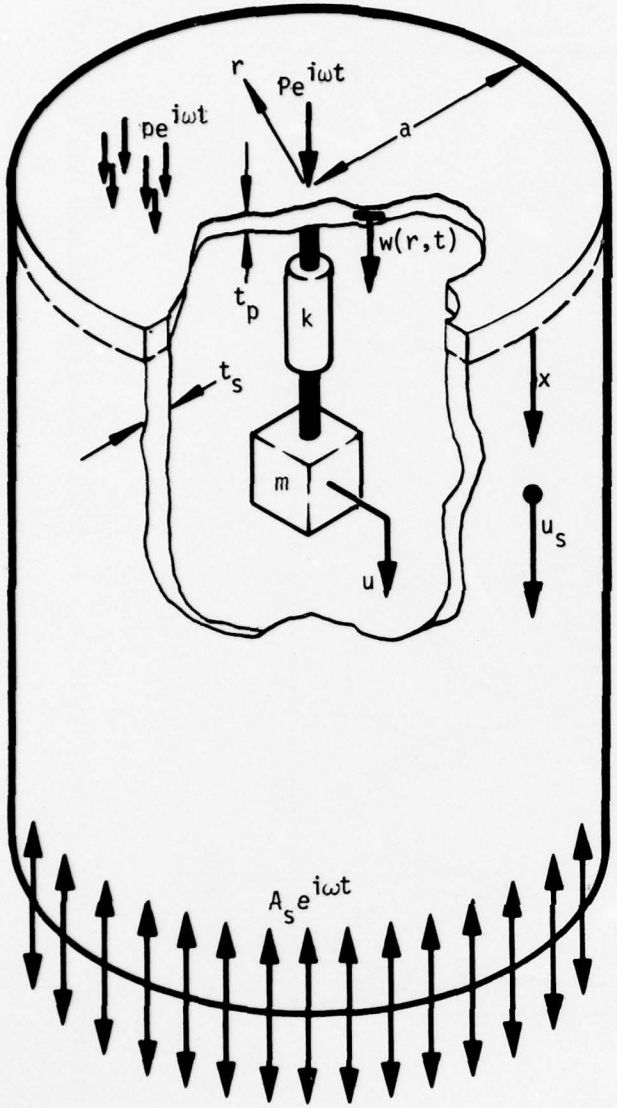

PLATE PROPERTIES E_p, t_p, ρ_p, Radius a

$D_p = E_p t_p^3 / 12\ (1-\nu^2)$

$\mu_p = \rho_p t_p$

SHELL PROPERTIES E_s, t_s, ρ_s

$c_s = \sqrt{E_s / \rho_s}$

EQUIPMENT Mass m

Spring Stiffness k

$\omega_o^2 = k/m$

Figure 7. Diagrammatic Representation of Silo-Like Structure with Attached Equipment

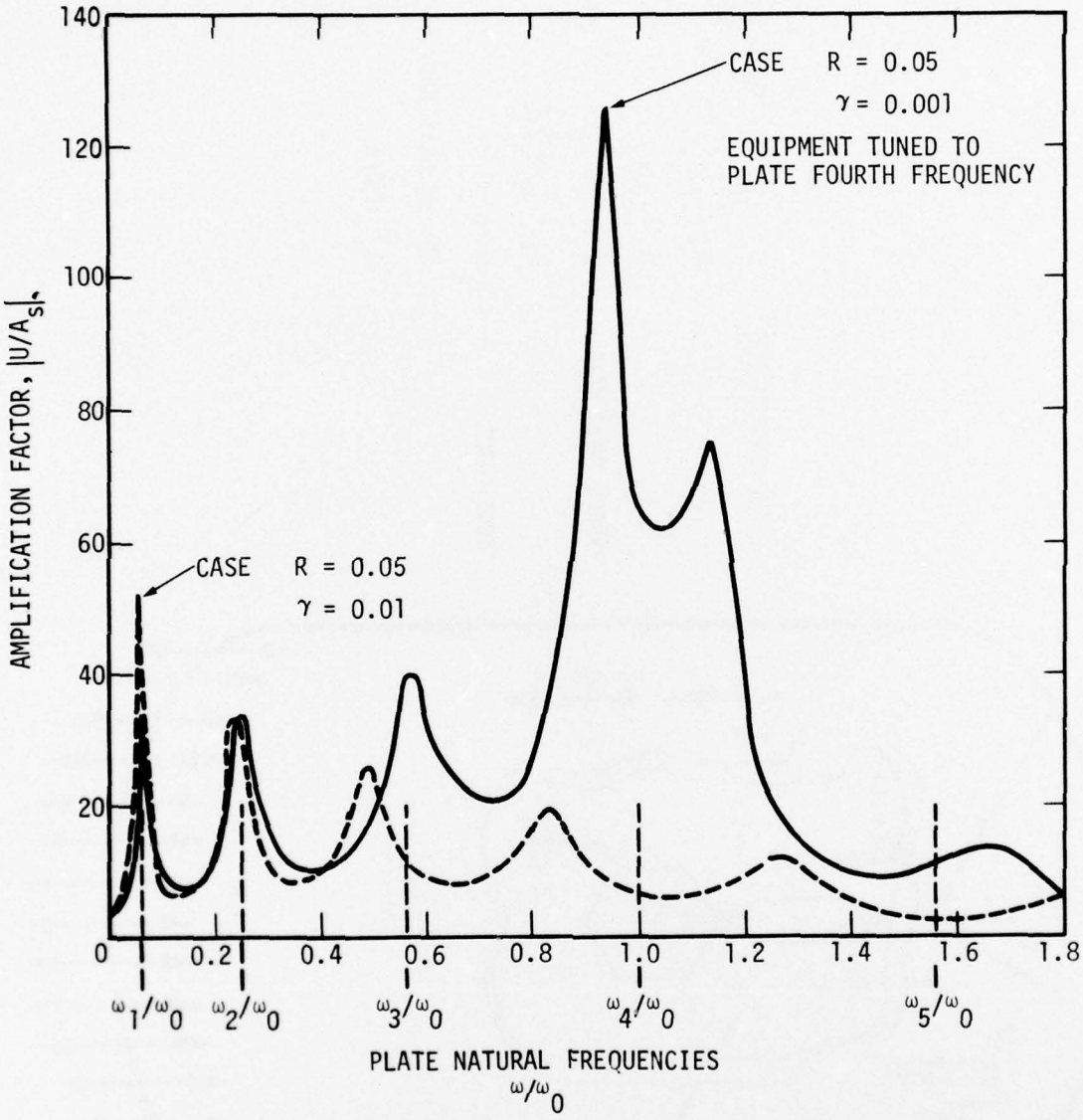

Figure 8. Amplification Factor as a Function of Non-Dimensional Frequency--Ground Shock Case

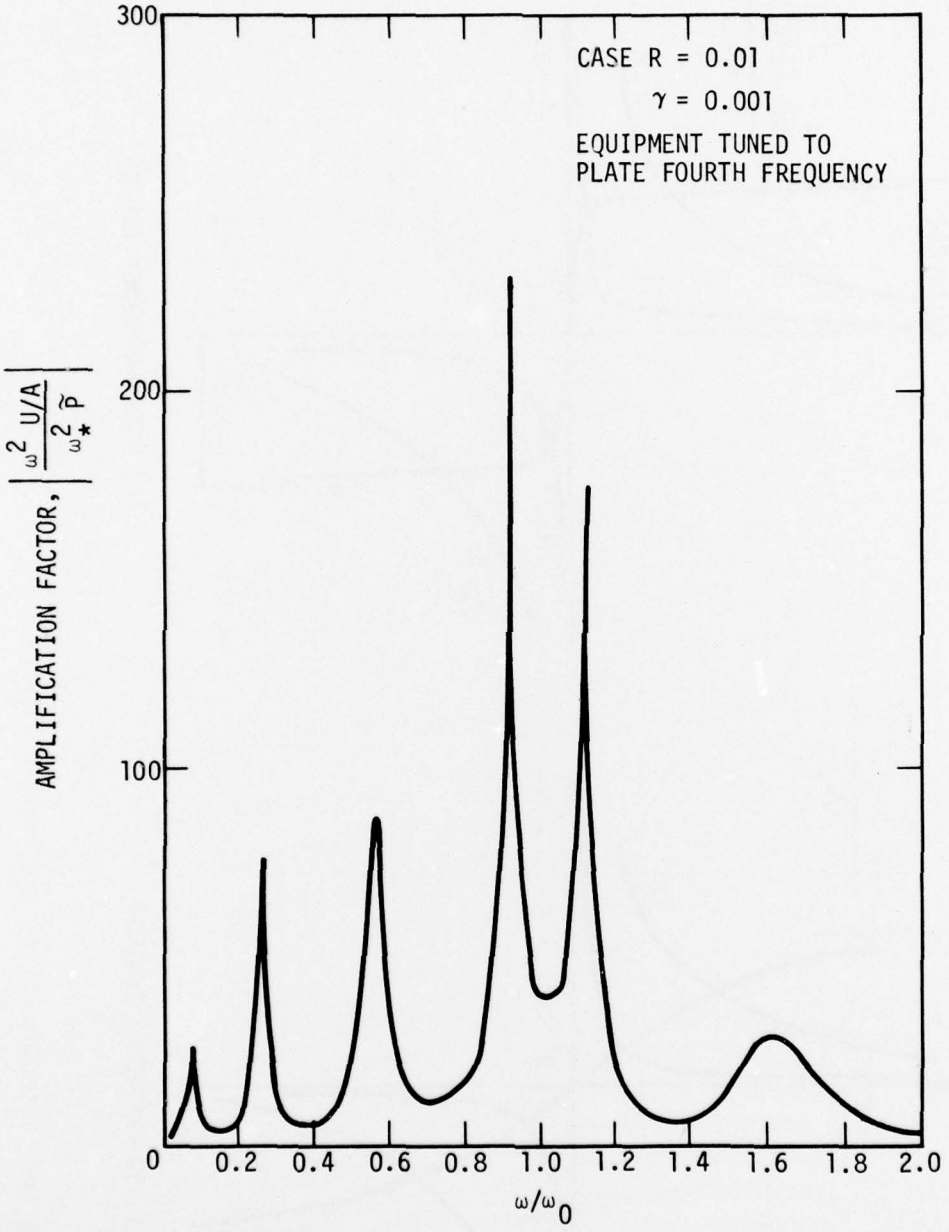

Figure 9. Amplification Factor as a Function of Non-Dimensional Frequency--Shaker Input

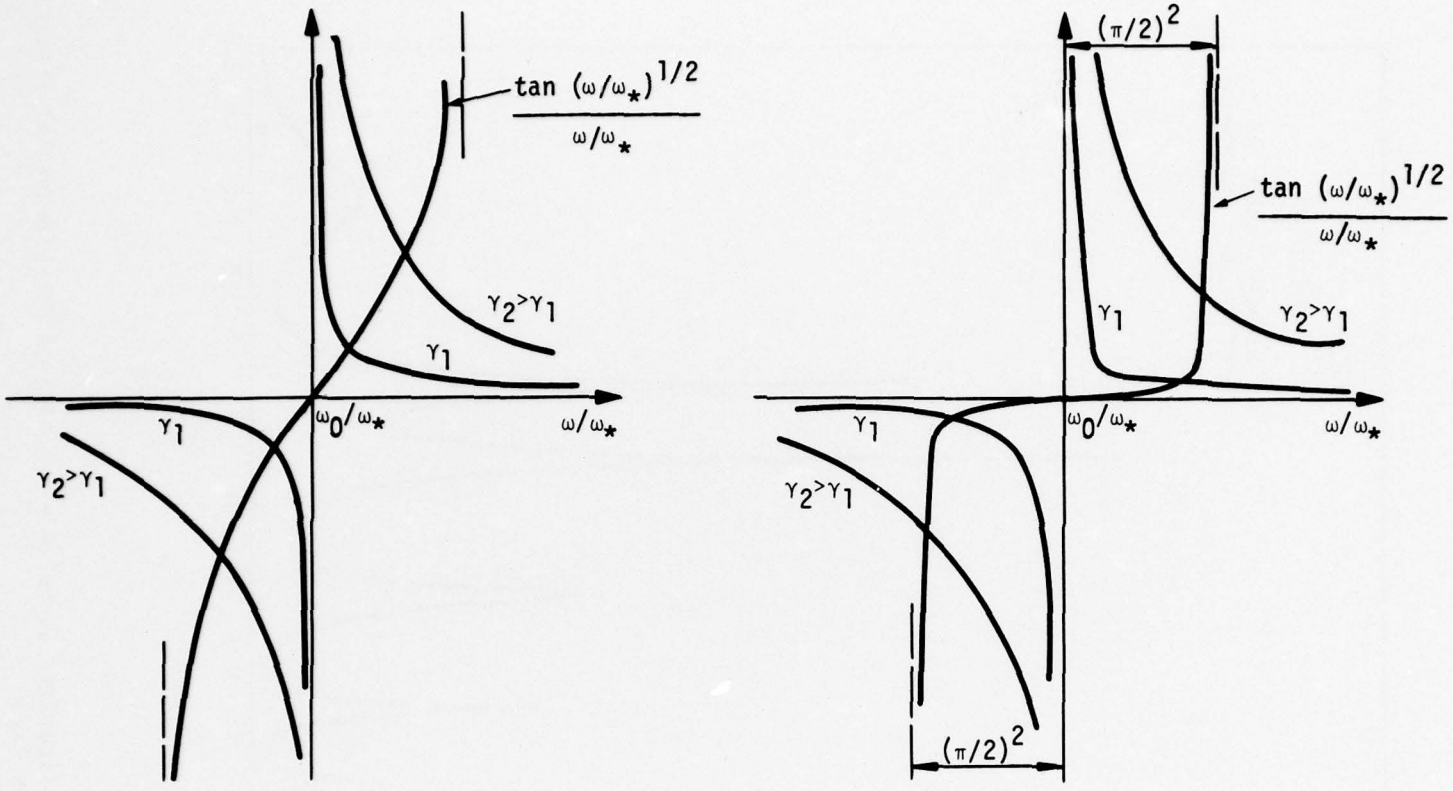

(a) LOW FREQUENCY TUNING

(b) HIGH FREQUENCY TUNING

Figure 10. Solution Curves for Tuned Resonance

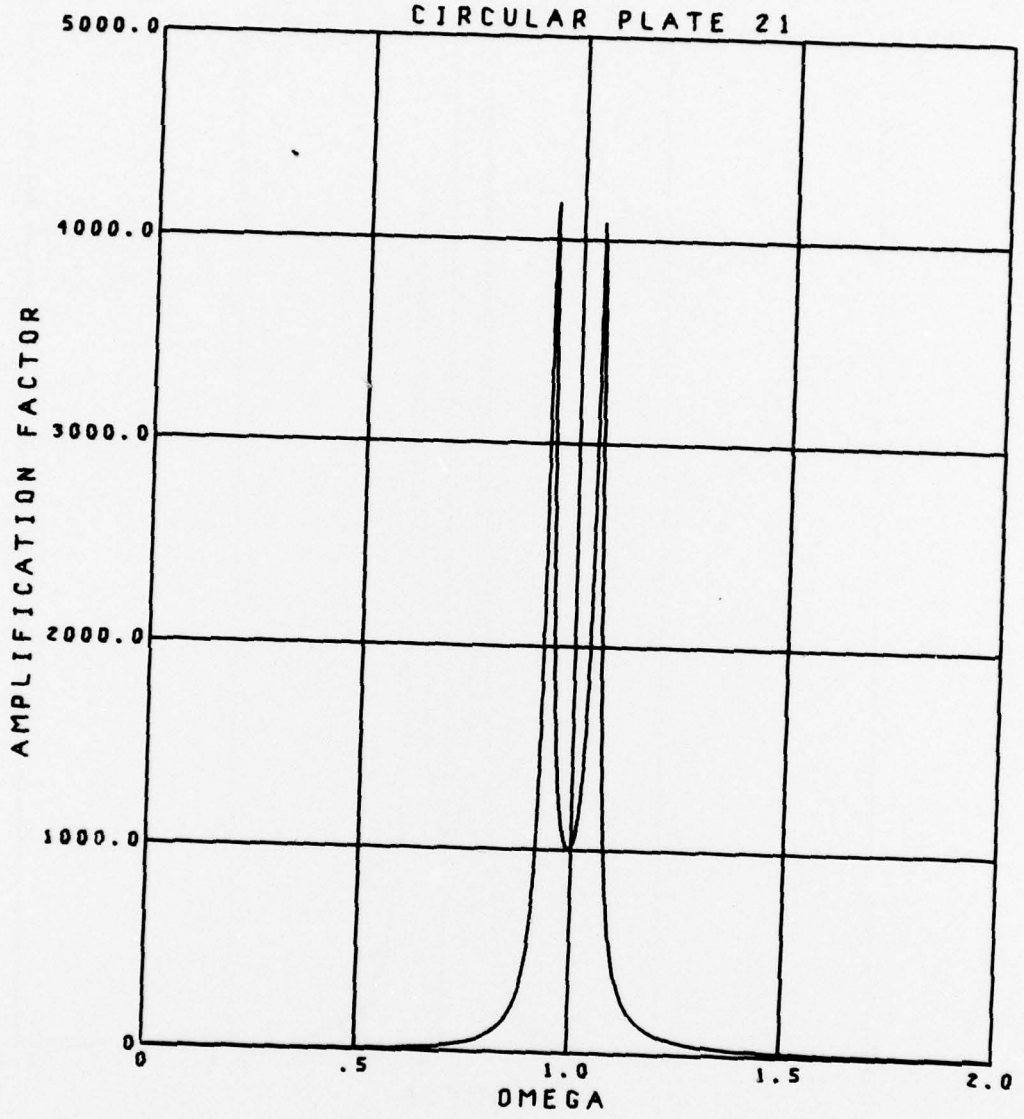

Figure 11a. Amplification Factor as a Function of Nondimensional Frequency for Shaker Problem with Equipment Tuned to Various Plate Frequencies. R = .01, γ = .001.

Equipment Tuned to First Plate Frequency

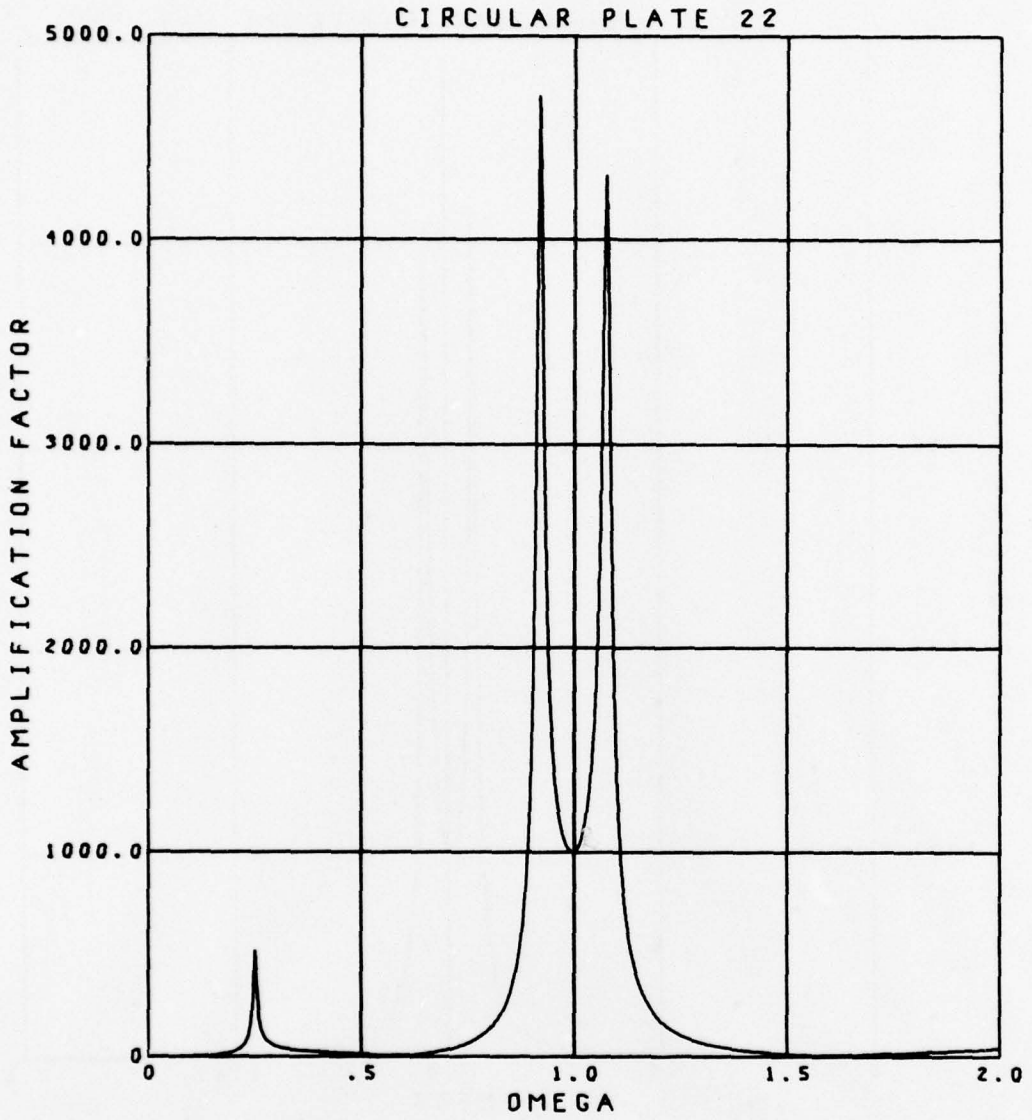

Figure 11b. Amplification Factor as a Function of Nondimensional Frequency for Shaker Problem with Equipment Tuned to Various Plate Frequencies. $R = .01$, $\gamma = .001$.

Equipment Tuned to Second Plate Frequency

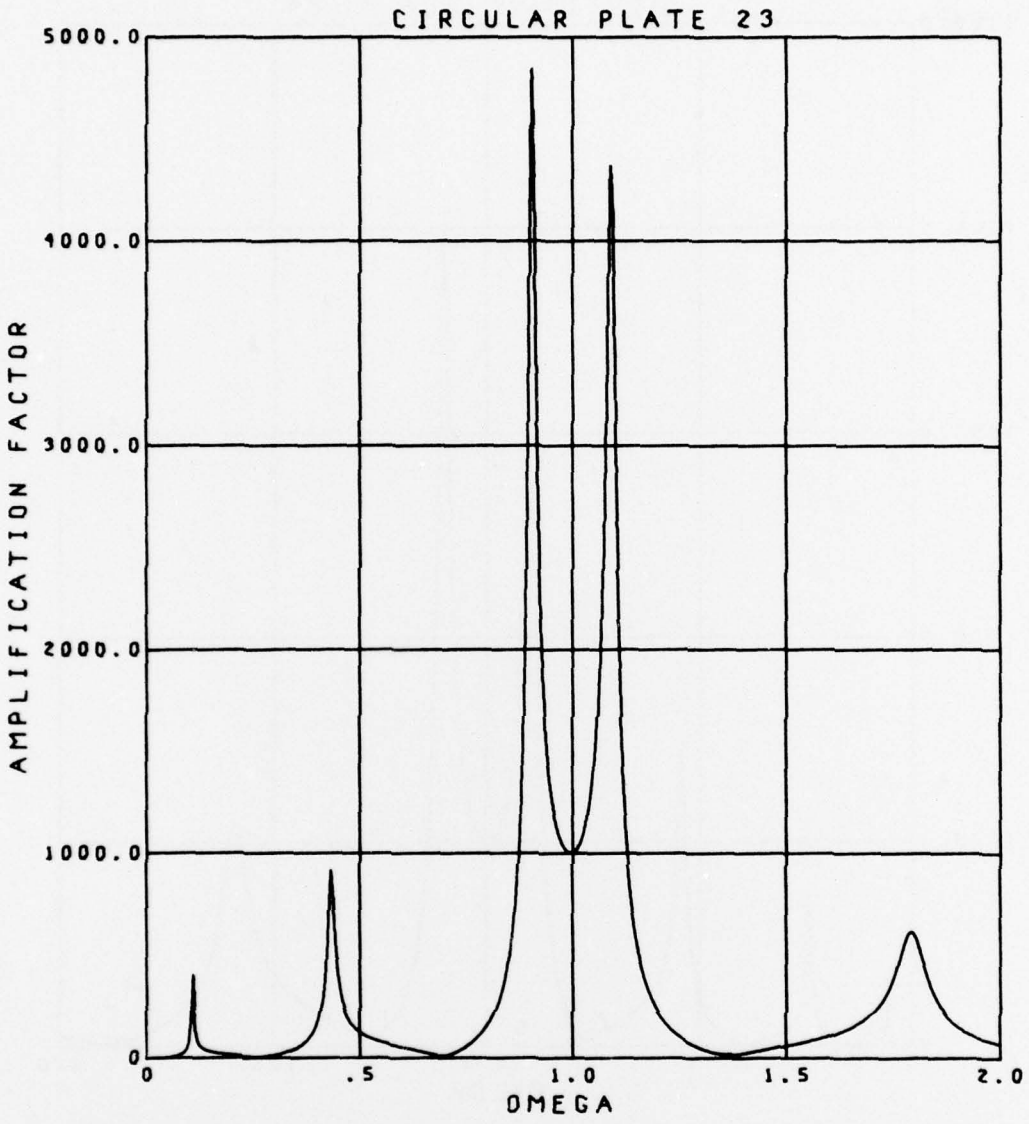

Figure 11c. Amplification Factor as a Function of Nondimensional Frequency for Shaker Problem with Equipment Tuned to Various Plate Frequencies. R = .01, γ = .001.

Equipment Tuned to Third Plate Frequency

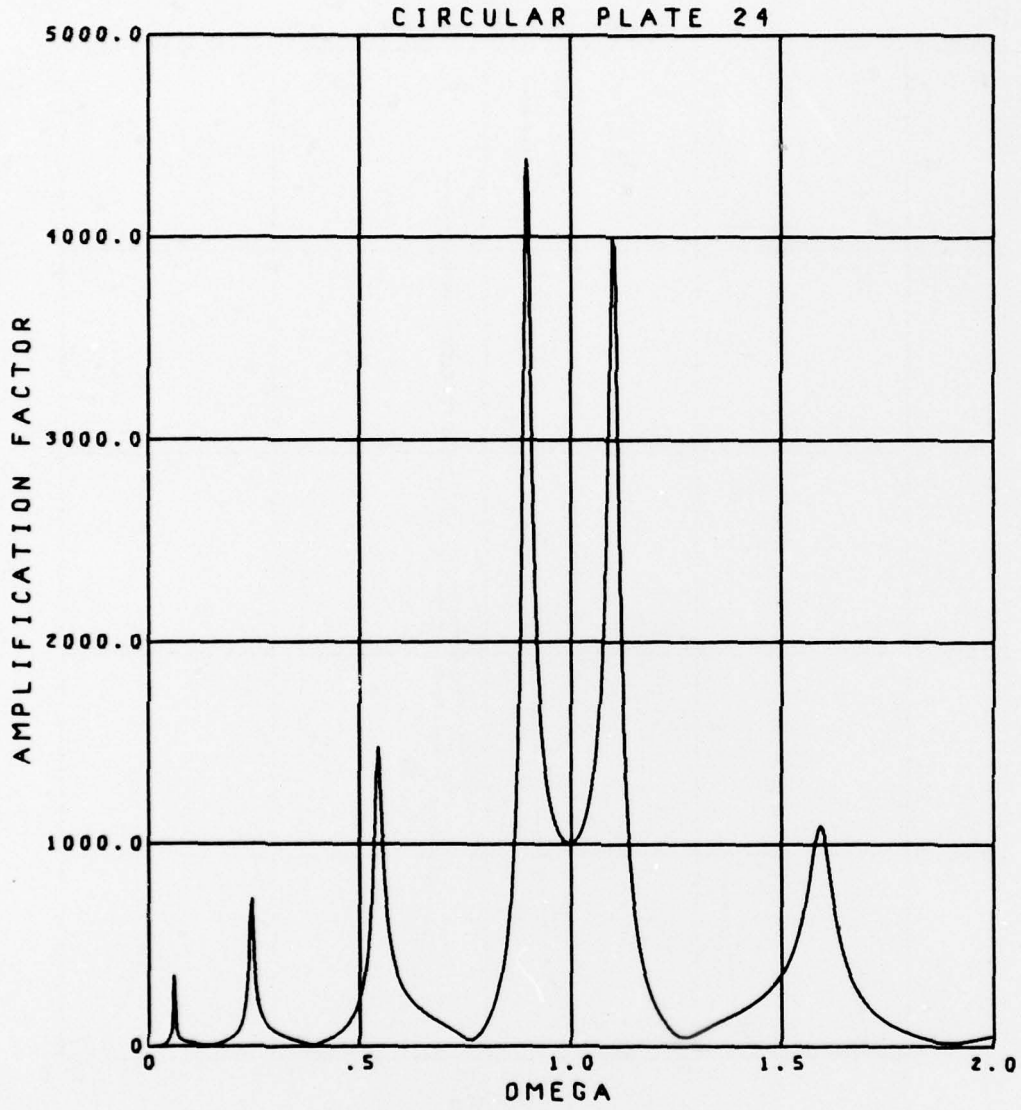

Figure 11d. Amplification Factor as a Function of Nondimensional Frequency for Shaker Problem with Equipment Tuned to Various Plate Frequencies. $R = .01$, $\gamma = .001$.

Equipment Tuned to Fourth Plate Frequency.

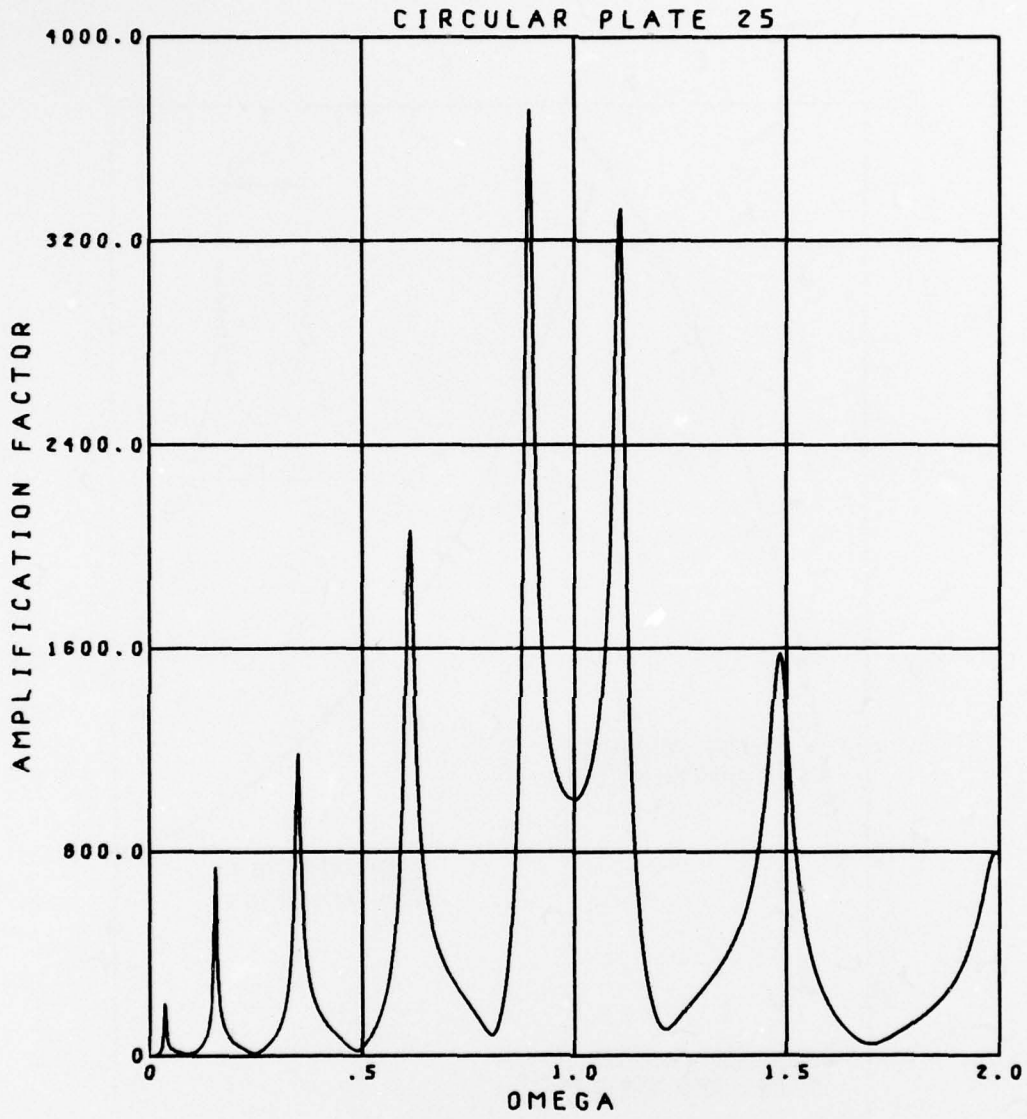

Figure 11e. Amplification Factor as a Function of Nondimensional Frequency for Shaker Problem with Equipment Tuned to Various Plate Frequencies. $R = .01$, $\gamma = .001$.

Equipment Tuned to Fifth Plate Frequency

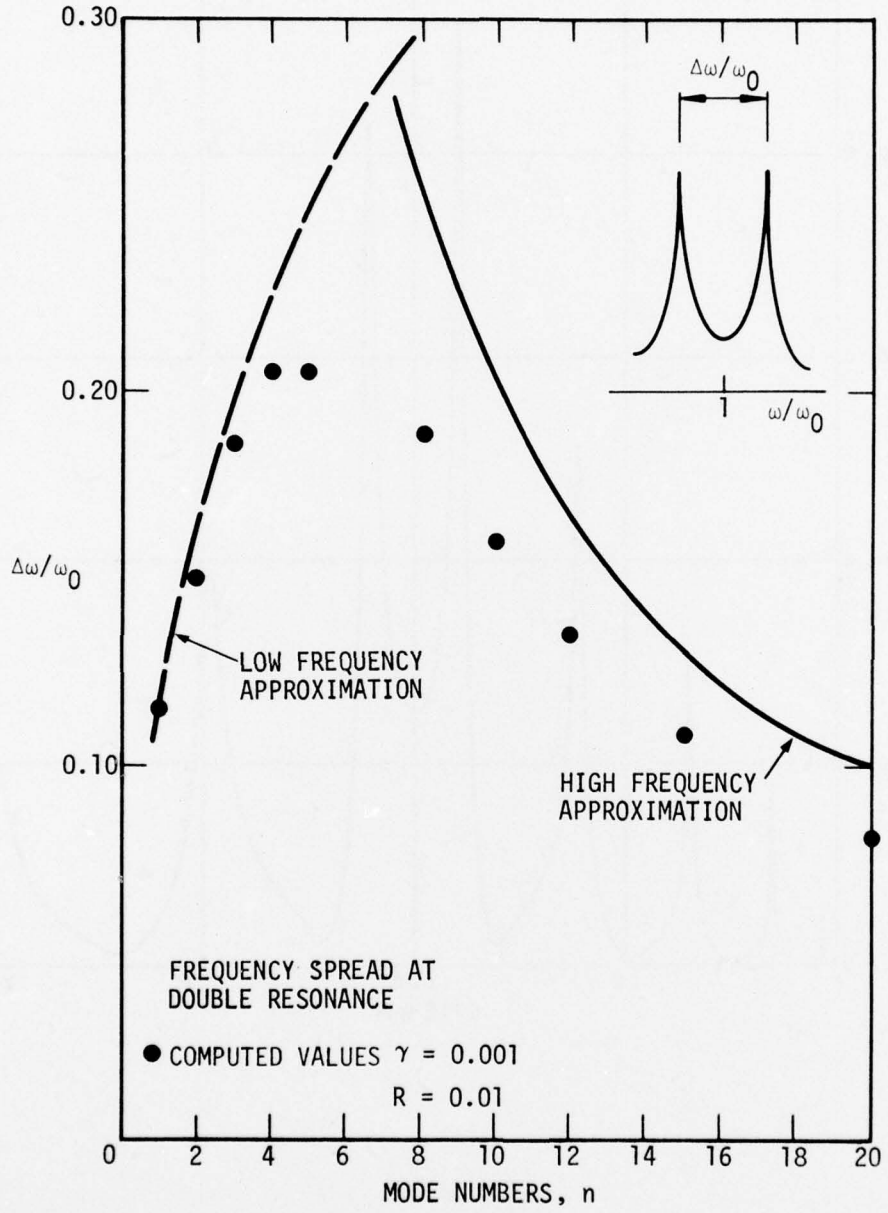

Figure 12. Frequency Spread at Double Resonance as a Function of the Mode Number to which the Equipment is Tuned

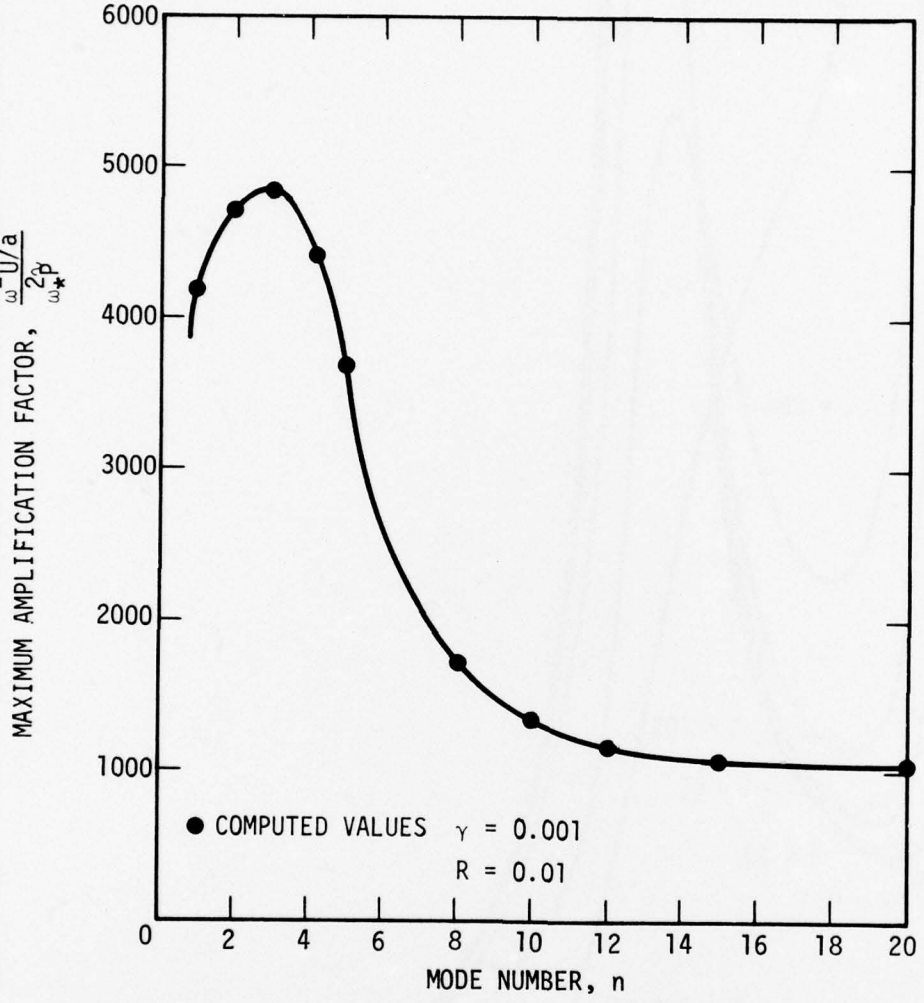

Figure 13. Maximum Amplitude of Double Resonance as a Function of the Mode Number to which the Equipment is Tuned

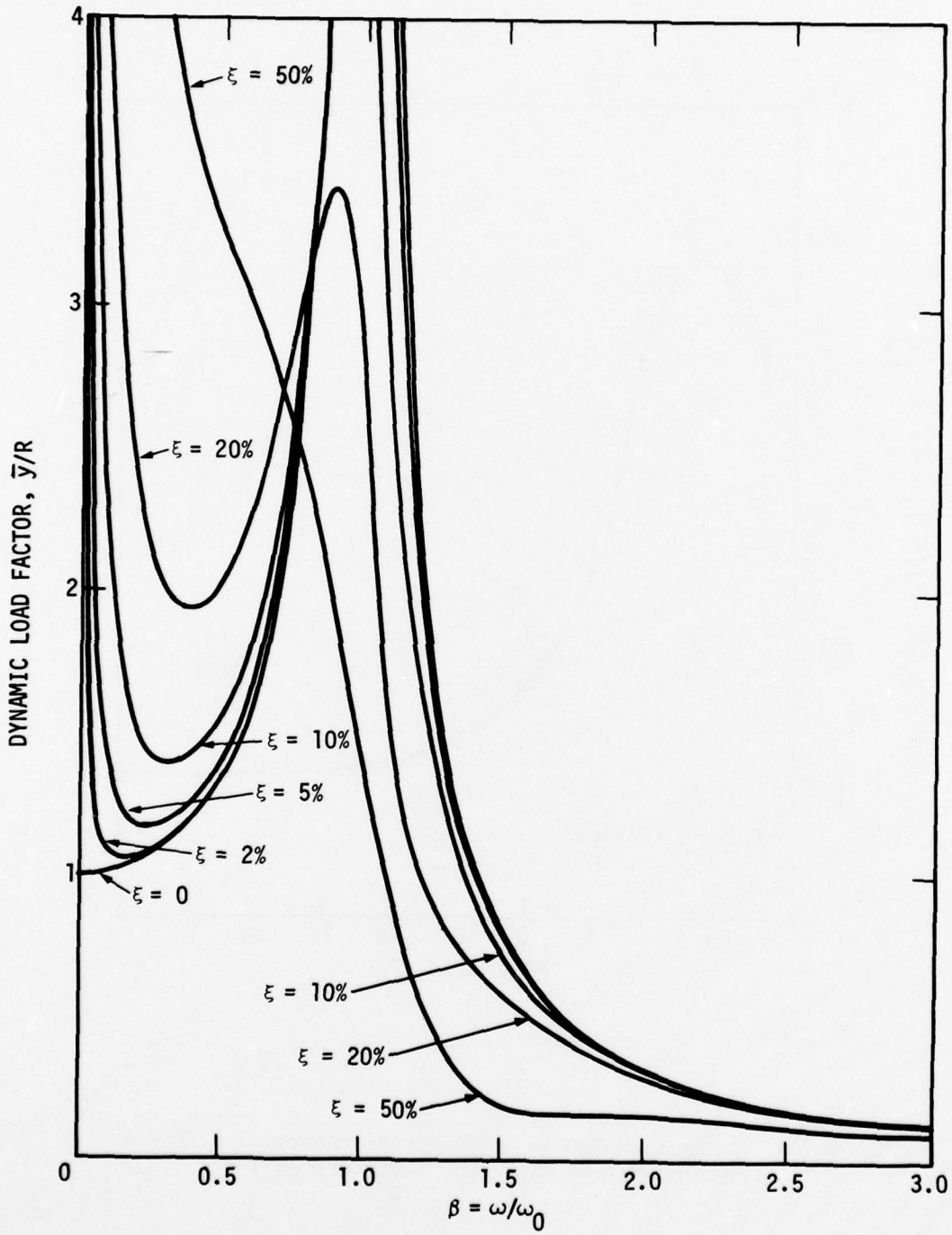

Figure 14. Dynamic Load Factor for Maxwell Model

DISTRIBUTION LIST

DEPARTMENT OF DEFENSE

Assistant Secretary of Defense
Cmd., Cont., Comm. & Intell.
ATTN: ODASD IA

Assistant to the Secretary of Defense
Atomic Energy
Department of Defense
ATTN: Honorable Donald R. Cotter
ATTN: Colonel R. N. Brodie

Director
Defense Advanced Rsch. Proj. Agency
ATTN: NMRO
ATTN: PMO
ATTN: STO
ATTN: Technical Library

Director
Defense Civil Preparedness Agency
Assistant Director for Research
ATTN: Staff Dir. Resr., George N. Sisson

Defense Documentation Center
Cameron Station
12 cy ATTN: TC

Director
Defense Intelligence Agency
ATTN: DB-4C2, Timothy [illegible]
ATTN: DB-4C1, Paul Castleberry
ATTN: DT-2, Wpns. & Sys. Div.
ATTN: Technical Library

Director
Defense Nuclear Agency
ATTN: DDST
3 cy ATTN: TITL, Tech. Library
2 cy ATTN: SPSS
ATTN: TISI, Archives

Dir. of Defense Rsch. & Engineering
Department of Defense
ATTN: S&SS (OS)

Commander
Field Command
Defense Nuclear Agency
ATTN: FCPR
ATTN: FCTMOF

Director
Joint Strat. Target Planning Staff, JCS
ATTN: DOXT
ATTN: XPFS
ATTN: JLTW-2
ATTN: STINFO, Library

Chief
Livermore Division, Field Command, DNA
Lawrence Livermore Laboratory
ATTN: FCPRL

DEPARTMENT OF DEFENSE (Continued)

Chief
Test Construction Division
Field Command Test Directorate
Defense Nuclear Agency
ATTN: FCTC

DEPARTMENT OF THE ARMY

Director
BMD Advanced Tech. Center
Huntsville Office
ATTN: CRDABH-S
ATTN: CRDABH-X

Program Manager
BMD Program Office
ATTN: CRDABM-NE

Commander
BMD System Command
ATTN: BDMSC-TEN, Noah J. Hurst

Director
Construction Engineering Rsch. Lab.
ATTN: CERL-SL

Dep. Chief of Staff for Rsch. Dev. & Acq.
Department of the Army
ATTN: Technical Library

Chief of Engineers
Department of the Army
ATTN: DAEN-RDM
ATTN: DAEN-MCE-D

Commander
Harry Diamond Laboratories
ATTN: DRXDO-NP

Commander
Picatinny Arsenal
ATTN: Technical Library

Director
US Army Ballistic Research Labs.
ATTN: DRXBR-X, Julius J. Meszaros
2 cy ATTN: Tech. Lib., Edward Baicy

Commander
US Army Communications Command
ATTN: Technical Library

Commander
US Army Electronics Command
ATTN: DRSEL-TL-IR, Edwin T. Hunter

Division Engineer
US Army Engineer Div. Huntsville
ATTN: HNDED-SR

Director
US Army Engr. Waterways Exper. Sta.
ATTN: Technical Library
2 cy ATTN: William Flathau/James Ballard

DEPARTMENT OF THE ARMY (Continued)

Commander
US Army Mobility Equip. R & D Center
ATTN: Technical Library

Commander
US Army Nuclear Agency
ATTN: ATCA-NAW
ATTN: Tech. Lib.

DEPARTMENT OF THE NAVY

Chief of Naval Research
Navy Department
ATTN: Technical Library
ATTN: Code 464, Jacob L. Warner/T. P. Quinn

Officer-in-Charge
Civil Engineering Laboratory
Naval Construction Battalion Center
ATTN: Technical Library
ATTN: R. J. Odello/S. Takahashi

Commander
David W. Taylor Naval Ship R & D Center
ATTN: Code L42-3, Library

Commander
Naval Electronic Systems Command
Naval Electronic Systems Command Hqs.
ATTN: PME 117-21A

Superintendent (Code 1424)
Naval Postgraduate School
ATTN: Code 2124, Tech. Rpts. Librarian

Director
Naval Research Laboratory
ATTN: Code 2600, Tech. Lib.

Commander
Naval Ship Engineering Center
Department of the Navy
ATTN: Technical Library

Commander
Naval Ship Rsch. & Development Center
Underwater Explosive Research Division
ATTN: Technical Library

Officer-in-Charge
Naval Surface Weapons Center
ATTN: Code WA501, Navy Nuc. Prgms. Off.
ATTN: Code 240, C. J. Aronson

Commander
Naval Surface Weapons Center
Dahlgren Laboratory
ATTN: Technical Library

President
Naval War College
ATTN: Technical Library

Commander
Naval Weapons Center
ATTN: Code 533, Tech. Lib.

DEPARTMENT OF THE NAVY (Continued)

Commanding Officer
naval Weapons Evaluation Facility
ATTN: Technical Library

DEPARTMENT OF THE AIR FORCE

AF Weapons Laboratory, AFSC
ATTN: DES, Lt Col Warren
ATTN: DE, Jimmie L. Bratton
ATTN: SUL

Headquarters
Air Force Systems Command
ATTN: Technical Library
ATTN: DLCAW

Assistant Secretary of the Air Force
Research & Development
Headquarters, US Air Force
ATTN: Colonel R. E. Steere

Deputy Chief of Staff
Research & Development
Headquarters, US Air Force
ATTN: Colonel J. L. Gilbert

Commander
Foreign Technology Division, AFSC
ATTN: PDBF, Mr. Spring
ATTN: NICD, Library
ATTN: ETDP
ATTN: PDBG

SAMSO/MN
ATTN: MNNH
ATTN: MMH

Commander in Chief
Strategic Air Command
ATTN: NRI-STINFO, Library
ATTN: XPFS

ENERGY RESEARCH & DEVELOPMENT ADMINISTRATION

Division of Military Application
US Energy Rsch. & Dev. Admin.
ATTN: Doc. Con. for Test Office

Sandia Laboratories
Livermore Laboratory
ATTN: Doc. Con. for Tech. Library

DEPARTMENT OF DEFENSE CONTRACTORS

Aerospace Corporation
2 cy ATTN: Tech. Info. Services
ATTN: Larry Selzer

Agbabian Associates
ATTN: Fred Safford/Lloyd Carlson
ATTN: M. Agbabian

Battelle Memorial Institute
ATTN: Technical Library

The BDM Corporation
ATTN: Technical Library

DEPARTMENT OF DEFENSE CONTRACTORS (Continued)

The Boeing Company
ATTN: Robert Dyrdahl
ATTN: Aerospace Library
ATTN: R. H. Carlson

Brown Engineering Company, Inc.
ATTN: Manu Patel

California Institute of Technology
ATTN: Thomas J. Ahrens

Civil/Nuclear Systems Corp.
ATTN: Robert Crawford

Gard, Incorporated
ATTN: G. L. Neidhardt

General Electric Company
TEMPO-Center for Advanced Studies
ATTN: DASIAC

IIT Research Institute
ATTN: R. E. Welch
ATTN: Technical Library

Lockheed Missiles & Space Company, Inc.
ATTN: Tom Geers, D/52-33, Bldg. 205

Martin Marietta Aerospace
Orlando Division
ATTN: G. Fotieo

McDonnell Douglas Corporation
ATTN: Robert W. Halprin

Merritt Cases, Incorporated
ATTN: J. L. Merritt
ATTN: Technical Library

DEPARTMENT OF DEFENSE CONTRACTORS (Continued)

The Mitre Corporation
ATTN: Library

Nathan M. Newmark
Consulting Engineering Services
B106A Civil Engineering Building
University of Illinois
ATTN: Nathan M. Newmark

Physics International Company
ATTN: Doc. Con. for Tech. Lib.

R & D Associates
ATTN: William B. Wright, Jr.
ATTN: Arlen Fields
ATTN: J. G. Lewis
ATTN: Technical Library
ATTN: Cyrus P. Knowles
ATTN: Albert L. Latter

The Rand Corporation
ATTN: C. C. Mow
ATTN: Technical Library

Science Applications, Inc.
ATTN: Technical Library

Science Applications, Inc.
ATTN: James Cramer

Southwest Research Institute
ATTN: A. B. Wenzel
ATTN: Wilfred E. Baker

Systems, Science & Software, Inc.
ATTN: Technical Library

TRW Defense & Space Sys. Group
ATTN: Tech. Info. Center/S-1930
ATTN: Pravin Bhutta, R1-1104
ATTN: Norm Lipner
2 cy ATTN: Peter K. Dai, R1/2170

TRW Defense & Space Sys. Group
San Bernardino Operations
ATTN: G. D. Hulcher

URS Research Company
ATTN: Technical Library

Weidlinger Assoc. Consulting Engineers
2 cy ATTN: Melvin L. Baron

Weidlinger Assoc. Consulting Engineers
3 cy ATTN: J. Isenberg
ATTN: J. M. Kelly
ATTN: J. L. Sackman